LegacyClimate 1.0: A dataset of pollen-based climate reconstructions from 2594 Northern Hemisphere sites covering the last 30 ka and beyond

Ulrike Herzschuh[1,2,3], Thomas Böhmer[1], Chenzhi Li[1,2], Manuel Chevalier[4,5], Raphaël Hébert[1], Anne Dallmeyer[6], Xianyong Cao[1,7], Nancy H. Bigelow[8], Larisa Nazarova[1,9], Elena Y. Novenko[10,11], Jungjae Park[12,13], Odile Peyron[14], Natalia A. Rudaya[15,16], Frank Schlütz[17,18], Lyudmila S. Shumilovskikh[18], Pavel E. Tarasov[19], Yongbo Wang[20], Ruilin Wen[21,22], Qinghai Xu[23], Zhuo Zheng[24,25]

[1] Polar Terrestrial Environmental Systems, Alfred Wegener Institute Helmholtz Centre for Polar and Marine Research, Telegrafenberg A45, 14473 Potsdam, Germany

[2] Institute of Environmental Science and Geography, University of Potsdam, Karl-Liebknecht-Str. 24-25, 14476 Potsdam, Germany

[3] Institute of Biochemistry and Biology, University of Potsdam, Karl-Liebknecht-Str. 24-25, 14476 Potsdam, Germany

[4] Institute of Geosciences, Sect. Meteorology, Rheinische Friedrich-Wilhelms-Universität Bonn, Auf dem Hügel 20, 53121 Bonn, Germany

[5] Institute of Earth Surface Dynamics IDYST, Faculté des Géosciences et l'Environnement, University of Lausanne, Bâtiment Géopolis, 1015 Lausanne, Switzerland

[6] Max Planck Institute for Meteorology, Bundesstrasse 53, 20146 Hamburg, Germany

[7] Alpine Paleoecology and Human Adaptation Group (ALPHA), State Key Laboratory of Tibetan Plateau Earth System, and Resources and Environment (TPESRE), Institute of Tibetan Plateau Research, Chinese Academy of Sciences, 100101 Beijing, China

[8] Alaska Quaternary Center, University of Alaska Fairbanks, Fairbanks, Alaska 99775, USA

[9] Kazan Federal University, Kremlyovskaya str. 18, 420008 Kazan, Russia

[10] Lomonosov Moscow State University, Faculty of geography, Leniskie gory 1, 119991 Moscow, Russia

[11] Department of Quaternary Paleogeography, Institute of Geography Russian Academy of Science, Staromonrtny lane, 29, 119017, Moscow, Russia

[12] Department of Geography, Seoul National University, 1 Gwanak-ro, Gwanak-gu, Seoul, 08826, Republic of Korea

[13] Institute for Korean Regional Studies, Seoul National University, 1 Gwanak-ro, Gwanak-gu, Seoul, 08826, Republic of Korea

[14] Institut des Sciences de l'Evolution de Montpellier, Université de Montpellier, CNRS UMR 5554, Montpellier, France

[15] PaleoData Lab, Institute of Archaeology and Ethnography, Siberian Branch, Russian Academy of Sciences, Pr. Akademika 36 Lavrentieva 17, 630090 Novosibirsk, Russia

[16] Biological Institute, Tomsk State University, Pr. Lenina, 26, Tomsk, 634050, Russia

[17] Lower Saxony Institute for Historical Coastal Research, D-26382 Wilhelmshaven, Germany

[18] Department of Palynology and Climate Dynamics, Albrecht-von-Haller Institute for Plant Sciences, University of Göttingen, Untere Karspüle 2, 37073 Göttingen, Germany

[19] Freie Universität Berlin, Institute of Geological Sciences, Palaeontology Section, Malteserstrasse 74-100, Building D, 12249 Berlin, Germany

[20] College of Resource Environment and Tourism, Capital Normal University, 105 West 3rd Ring Rd N, 100048 Beijing, China

[21] Key Laboratory of Cenozoic Geology and Environment, Institute of Geology and Geophysics, Chinese Academy of Sciences, 19 Beitucheng West Road, Chaoyang District, 100029 Beijing, China

[22] CAS Center for Excellence in Life and Paleoenvironment, 100044 Beijing, China

[23] School of Geographic Sciences, Hebei Normal University, 050024 Shijiazhuang, China

[24] Guangdong Key Lab of Geodynamics and Geohazards, School of Earth Sciences and Engineering, Sun Yat-sen University, 519082 Zhuhai, China

[25] Southern Marine Science and Engineering Guangdong Laboratory (Zhuhai), 519082 Zhuhai, China

Correspondence: Ulrike Herzschuh (Ulrike.Herzschuh@awi.de)

Abstract. Here we describe the LegacyClimate 1.0, a dataset of the reconstruction of mean July temperature (T_{July}), mean annual temperature (T_{ann}), and annual precipitation (P_{ann}) from 2594 fossil pollen records from the Northern Hemisphere spanning the entire Holocene with some records reaching back to the Last Glacial. Two reconstruction methods, the Modern Analogue Technique (MAT) and Weighted-Averaging Partial-Least Squares regression (WA-PLS) reveal similar results regarding spatial and temporal patterns. To reduce the impact of precipitation on temperature reconstruction and vice versa, we also provide reconstructions using tailored modern pollen data limiting the range of the corresponding other climate variables. We assess the reliability of the reconstructions using information from the spatial distributions of the root-mean-squared error of prediction and reconstruction significance tests. The dataset is beneficial for synthesis studies of proxy-based reconstructions and to evaluate the output of climate models and thus help to improve the models themselves. We provide our compilation of reconstructed T_{July}, T_{ann}, and P_{ann} as open-access datasets at PANGAEA (https://doi.pangaea.de/10.1594/PANGAEA.930512; Herzschuh et al., 2021). R code for the reconstructions is provided at Zenodo (https://doi.org/10.5281/zenodo.5910989; Herzschuh et al., 2022b), including harmonized open-access modern and fossil datasets used for the reconstructions, so that customized reconstructions can be easily established.

1 Introduction

The comparison of climate model outputs with climate data is essential for model improvements (Eyring et al., 2019). The extratropical Northern Hemisphere is of particular interest because it is known for complex spatial and temporal temperature and precipitation patterns. However, the period for which instrumental observations are available is only of limited use to validate simulations in particular when assessing climate response to natural climate drivers because it is too short and because it is impacted by human-induced greenhouse gas forcing. Climate proxy data derived from natural archives are therefore of great value.

Previous proxy-based climate inferences have contributed to major debates about Holocene climate change. For example, while simulations indicate gradual warming of the Holocene, temperature proxy data syntheses rather support a mid-Holocene optimum which resulted in the “Holocene conundrum” debate (Liu et al., 2014). Qualitative proxy-based inferences indicate that the mid-Holocene in the Northern Hemisphere mid-latitudes was rather dry and warm compared with present-day in agreement with modelling outputs (Routson et al., 2019). Also, quantitative precipitation reconstructions from Eastern and Central Asia unveiled the complex monsoon-westerlies interactions (Chen et al., 2019; Herzschuh et al., 2019).

Fossil pollen records are well-established in their use as a palaeoecological and palaeoclimatological proxy and of great value as indicators of past environmental and climatic change for many decades. Considerable efforts have been made to establish regional, continental and even global data repositories like the North American Pollen Database (NAPD; https://www.ncei.noaa.gov/products/paleoclimatology, last access: 1 July 2020), the European Pollen Database (EPD; http://www.europeanpollendatabase.net/index.php, last access: 1 July 2020) and the Neotoma Paleoecology Database (https://www.neotomadb.org/, last access: 1 April 2021; Williams et al., 2018). Pollen data from archives across multiple environmental settings such as lakes, wetlands, or marine sediments, have been widely used to quantitatively reconstruct past vegetation and climate variables (Birks, 2019; Chevalier et al., 2020). Pollen data are the only land-derived proxy data that have sufficient temporal and spatial coverage to allow for climate model evaluation of the late Quaternary period. A number of methods have been proposed for making pollen-based climate reconstructions (Chevalier et al., 2020): among them, classification approaches like the Modern Analogue Technique (MAT) or regression approaches like Weighted-Averaging Partial-Least Squares regression (WA-PLS) are most commonly used. MAT and WA-PLS rely on extensive collections of modern training data. Designing a robust calibration dataset from modern pollen assemblages is a crucial part of the reconstruction process. A suitable calibration dataset should cover a wide range of climatic and environmental gradients in order to represent an empirical relationship between pollen assemblages and climate (Birks et al., 2010; Chevalier et al., 2020). Like with fossil pollen records, data syntheses and repositories also exist for modern surface pollen data e.g. for North America (Whitmore et al., 2005), Eurasia (Davis et al., 2013 and 2020) and China (Cao et al., 2013; Herzschuh et al., 2019).

For temperature reconstruction time-series, several broad-scale syntheses exist; however, either they originate from different proxies (Kaufman et al., 2020a and 2020b) or are restricted to certain continents or regions or/and are poorly documented (Mauri et al., 2015; Marsicek et al., 2018; Routson et al., 2019). Temperature reconstructions from extratropical Asia are mostly lacking. Precipitation syntheses are available from Europe (Mauri et al., 2015), North America (Gajewski, 2000) and China and Mongolia (Herzschuh et al., 2019) but, hitherto, no global or hemispheric syntheses of quantitative precipitation changes are available for the Holocene.

In a recent effort, we synthesized and taxonomically harmonized pollen records available in the Neotoma Paleoecology Database (Williams et al., 2018) and additional records from China and Siberia (Cao et al., 2013 and 2020) into a global Late Quaternary fossil pollen dataset (LegacyPollen 1.0; Herzschuh et al., 2022c) and revised all chronologies of those records using a Bayesian approach that allows for the inference of temporal uncertainties (LegacyAge 1.0; Li et al., 2022). Here, in the third part of interconnected studies, we present the pollen-based reconstruction of mean July temperature (T_{July}), mean annual temperature (T_{ann}) and annual precipitation (P_{ann}) including reconstruction and temporal uncertainties as well as quality measures from 2594 records from the Northern Hemisphere using WA-PLS and MAT (LegacyClimate 1.0; this study).

2 Methods

2.1 Input data

The objective of this study is to create a dataset of quantitative reconstructions of T_{July}, T_{ann} and P_{ann} spanning the last 30 ka and beyond from fossil pollen records. These variables (or variables highly correlated to them) were shown to explain most variance in the modern pollen data (T_{July}, P_{ann}) or are typically used in synthesis studies (T_{ann}). We used fossil data set compiled in LegacyPollen 1.0 (stored on the PANGAEA open database and presented in Herzschuh et al. (2022c) that integrates pollen records archived in Neotoma Paleoecology Database, a dataset from Eastern and Central Asia (Cao et al., 2013; Herzschuh et al., 2019) and a dataset from Northern Asia (Cao et al., 2020). Ages were taken from the “Bacon” (Blaauw and Christen, 2011) age-depth models presented in Li et al. (2022, LegacyAge 1.0), and for each record, we provide an ensemble of 1000 realizations of the age-depth model in our data product so that it can be used to account for chronological uncertainty on the reconstructions.

We compiled the fossil data into four sub-continental datasets for Eastern North America (<104°W; Williams et al., 2000), Western North America, Europe and Asia. We restricted the analyses to the 70 most common taxa on each continent to reduce computational power after making sure that higher taxa number would not substantially improve model statistics in climate reconstructions. To identify the most common taxa we used Hill´s N2 diversity index (i.e., the effective number of occurrences of a species in the dataset; Hill, 1973). For all analyses, square-root percentages were used if not indicated otherwise.

A modern pollen training dataset comprised of 15379 sites includes datasets from Eurasia (EMPD1, Davis et al. 2013; EMPD2, Davis et al. 2020; Herzschuh et al., 2019; Tarasov et al., 2011) and North America (Whitmore et al., 2005). The modern pollen datasets were taxonomically harmonized in accordance with the fossil pollen dataset (see details in Herzschuh et al., 2022c).

The site-specific T_{ann}, T_{July}, P_{ann} were derived from WorldClim 2 version 2.1 (spatial resolution of 30 seconds (~1 km2), https://www.worldclim.org, Fick and Hijmans, 2017) by extracting the climate data at the location of the modern sample sites using the *raster* package in R (version 3.5-11, Hijmans et al., 2021; R Core Team, 2020). The WorldClim 2 dataset provides spatially interpolated gridded climate data aggregated from weather stations as temporal averages between 1970-2000 (Fick and Hijmans, 2017). We used monthly average temperature data to extract the mean T_{July} and the "bioclimatic variables" bio1 (T_{ann}) and bio12 (P_{ann}).

2.2 Reconstruction methods

Our reconstruction approach included MAT (Overpeck et al., 1985) and WA-PLS (ter Braak and Juggins, 1993) by applying the MAT and WAPLS functions from the *rioja* package (version 0.9-21, Juggins, 2019) for R (R Core Team, 2020) on our Northern Hemispheric fossil pollen synthesis. For each fossil location, we calculated the geographic distance between each modern sampling site and the fossil pollen record using the *rdist.earth* function from the *fields* R-package (version 10.3, Nychka et al., 2020) and selected a unique calibration set from modern sites within a 2000 km radius. We fixed the radius to 2000 km, instead of 1500 km as suggested from a study in Eastern Asia by Cao et al. (2017), because the modern dataset density is rather low in Northern Asia. For the reconstruction with MAT, we used the original pollen percentages of the selected fossil pollen taxa, looking for 7 analogues between the pollen data

and the selected calibration dataset. The dissimilarity between the fossil samples and the modern pollen assemblages was determined by squared-chord distance of the percentage data (Simpson, 2012; Cao et al., 2014).

In addition to the classic WA-PLS reconstruction, we also propose WA-PLS_tailored. This approach addresses the problem that co-variation of climate variables today in space is transferred to the reconstruction even if the past temporal relationship among the climate variables mechanistically differs. In fact, this approach aims to make use of the full climate space covered by the modern pollen samples avoiding those samples in the calibration set that cause spatial covariation. This approach is based on the assumption that several climate variables can be reflected in one and the same pollen assemblage because different plant taxa have different optima in temperature and precipitation ranges and might therefore occur with different co-occurrence and abundance pattern. To reconstruct T_{July} we identified the P_{ann} range reconstructed by WA-PLS and extended it by 25% to both ends of the modern P_{ann} range in order to reduce the influence of P_{ann} on T_{ann} and T_{July} reconstruction due to co-variation. We applied the same method to the reconstruction of P_{ann}. T_{ann} and T_{July} were tailored by P_{ann}; P_{ann} was tailored by T_{July} and, additionally, by T_{ann} (illustrated for an example in Appendix Fig. 1). Reconstruction uncertainties are provided as root mean square errors (RMSE) derived from the output in the MAT and WAPLS functions. Model errors of WA-PLS and MAT are reported as root mean square error of prediction (RMSEP) derived from leave-one-out cross-validation.

We provide site- or sample-specific measures of quality in addition to the error estimates and model statistics to allow the user to assess the quality of the climate reconstruction dataset. First, we applied a Canonical Correlation Analysis (CCA) to the modern training dataset in order to explore the modern relationship between the pollen spectra and the climate variables and to infer the explained variance in the modern pollen dataset by the target climate variables (ter Braak, 1988) by using the *cca* function in the *vegan* R-package (version 2.5-7, Oksanen et al., 2020). The ratio between constrained (λ_1) and unconstrained (λ_2) explained variance was determined for all modern training datasets used for climate reconstructions. High values of λ_1 vs λ_2 are commonly considered as an indicator to measure how well the target environmental variable is strongly related to the variation in the modern pollen data set (e.g. Juggins, 2012).To infer the analogue quality as an indicator of no-analogue situations we calculated the minimum dissimilarity (squared chord distance) between modern pollen assemblages and fossil pollen

192 assemblages with probability thresholds of 1%, 2.5% and 5% using the *minDC* function from the
193 *analogue* R-package (version 0.17-6, Simpson et al., 2021).

194 A statistical significance test (Telford and Birks, 2011) was applied using the *randomTF* function in the
195 *palaeoSig* R-package (version 2.0-3, Telford, 2019). In this test, the proportion of variance in the fossil
196 pollen data explained by the reconstructed environmental variable is estimated from redundancy
197 analysis (RDA) and tested against a null distribution generated from a total of 999 randomly generated
198 environmental variables from the training data. A reconstruction is considered statistically significant if
199 the reconstructed variable explains more of the variance than 95% of the random reconstructions
200 (Telford and Birks, 2011). The reconstructed climate parameters were tested as introducing the
201 environmental variable as a single variable in a run, as well as with partialling out the explained variance
202 in the pollen data by the respective other variables.

203 We used Plantaginaceae (mostly representing *Plantago lanceolata*-type in Europe) and *Rumex*-type to
204 assess human influence as an indicator for intense herding (Behre, 1988). In addition, we calculated the
205 correlation between the WA-PLS reconstruction of T_{July}, T_{ann} and P_{ann} and the pollen percentages of
206 Plantaginaceae and *Rumex* for 9000, 3000 and 1000 years BP.

207

208 **3 Dataset description LegacyClimate 1.0: input data, reconstructions and reconstruction model**
209 **statistics**

210 LegacyClimate 1.0 provides pollen-based reconstructions and sample-specific reconstruction errors of
211 T_{ann}, T_{July} and P_{ann} for 2594 fossil pollen records (i.e., a total of 146067 single pollen samples) from three
212 reconstruction methods (WA-PLS, WA-PLS_tailored, MAT). Furthermore, we provide the method-
213 specific model metadata and quality measures for each record and each climate variable (Table 1). To
214 ease data handling, the dataset files are separated into Western North America, Eastern North America,
215 Europe and Asia.

216

217 **Table 1.** Structure and content of the LegacyClimate 1.0 data with details about the information
218 contained in the input datasets, in the climate reconstructions and the reconstruction model statistics.

219

220

Datasets	Content
Input datasets	Modern pollen dataset of 15379 sites Modern dataset of T_{ann}, T_{July}, P_{ann} Fossil pollen data (LegacyPollen 1.0) for 2594 sites with a total of 146067 samples Bacon age-depth models (LegacyAge 1.0) for 2579 sites
LegacyClimate 1.0: Climate reconstructions	Reconstructions and sample-specific reconstruction errors of T_{ann}, T_{July} and P_{ann} for 2594 sites using MAT, WA-PLS and WA-PLS_tailored Ensemble of 1000 realizations of the Bacon age-depth models for 2579 sites
LegacyClimate 1.0: Reconstruction model statistics	**Site information** (Event label, Source, ID, Site name, Longitude, Latitude) **Modern pollen dataset information** (number of modern analogues, range of climate variables) **Model statistics for each site for MAT**, **WA-PLS, WA-PLS_tailored** (including r^2 observed vs. predicted, RMSEP, no. of WA-PLS components)

LegacyClimate 1.0: Quality Measures	**Canonical Correlation Analysis (CCA)** of the modern training dataset **Minimum dissimilarities** between modern pollen assemblages and fossil pollen assemblages for each site for MAT **Statistical significances** sensu Telford & Birks (2011) for each site for MAT, WA-PLS, WA-PLS_tailored

4 Dataset assessment

4.1 Spatial and temporal coverage of LegacyClimate 1.0

In total, we provide reconstructions for 2594 fossil pollen records. Among them 670 records are located from Eastern North America, 361 records from Western North America, 1075 records from Europe and 488 Asian records (Fig. 1). The temporal coverage of the records is rather uneven: 119 and 289 records cover the periods before 30,000 years (Fig. 2) and the Last Glacial Maximum, respectively. A total of 1229, 1845 and 2052 records are available for 12-11 ka, 6-5 ka BP and 2-1 ka BP, respectively.

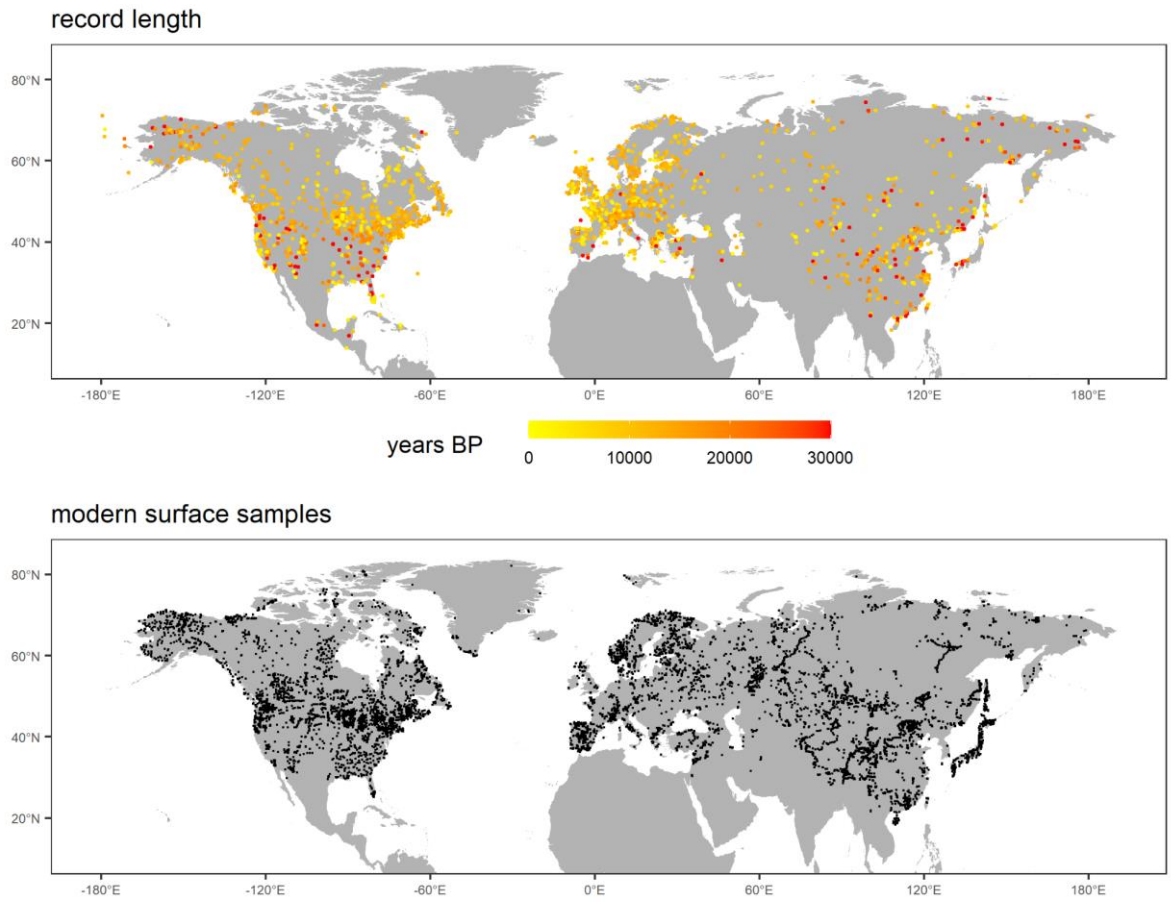

Figure 1. Top: map indicating the spatial distribution and record lengths covered by the LegacyPollen 1.0 dataset (Herzschuh et al., 2022c) for which climate reconstructions, temporal and reconstruction uncertainties and reconstruction quality measures are provided in LegacyClimate 1.0 with a total of 2594 records; Bottom: spatial distribution of modern pollen dataset used for reconstruction with a total of 15379 sites.

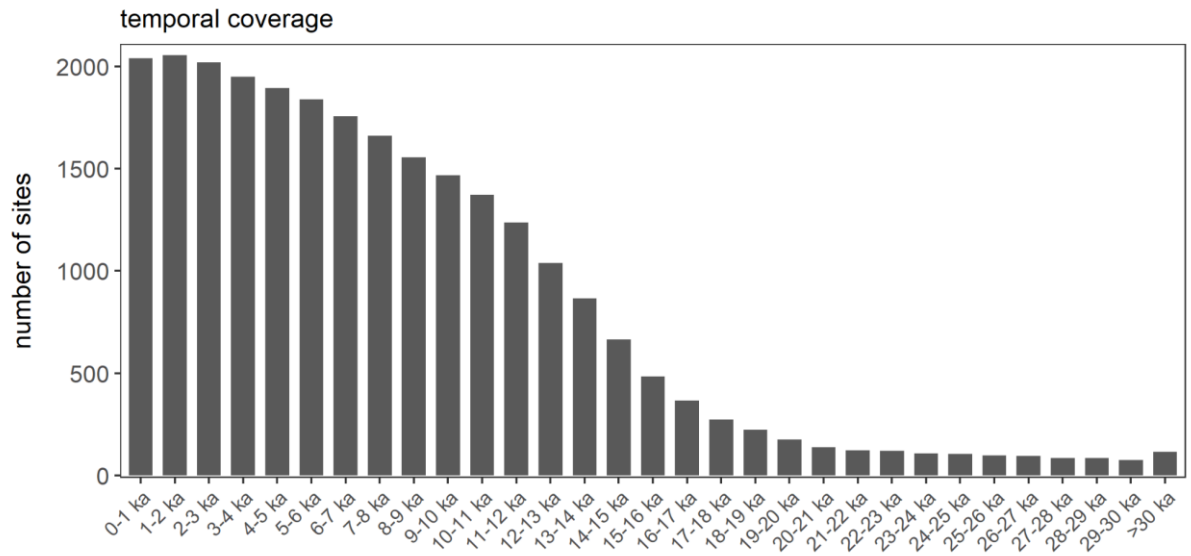

Figure 2. Number of records that cover certain millennia of the last 30 ka.

4.2 Modern relationships between pollen and climate assessed by constrained ordination.

Results from CCA applied to modern datasets reveal that T_{July}-constrained ordinations have high λ_1/λ_2 ratios, indicating a strong relationship between this climate variable and modern pollen assemblages, in Eastern North America while low ratios can be found in Central Asia. The spatial pattern of λ_1/λ_2 of ordinations constrained by T_{ann} is overall similar to those of T_{July} but the ratios are slightly higher for T_{ann} than for T_{July}. Reconstructions for P_{ann} show low ratios in Europe and Eastern North America. Areas with high ratios are concentrated in Alaska and East Asia (Fig. 3).

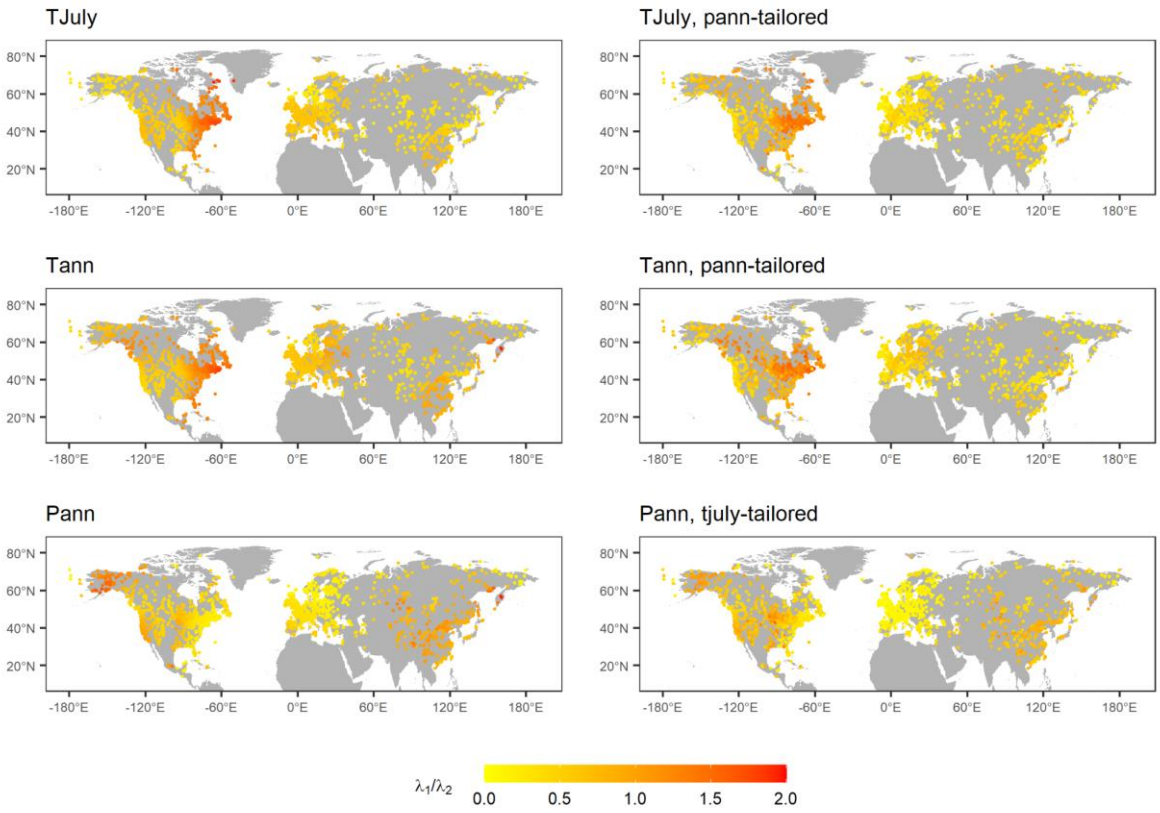

246

247 **Figure 3.** Maps showing λ_1/λ_2, representing the ratio of explained variance of first axis (constrained) vs.
248 second (unconstrained) axis as revealed by applying a CCA to all modern training datasets that were
249 used for the reconstructions. High ratios (>1) indicate a strong relationship between the modern pollen
250 datasets and climate. Constraining variables as well as tailoring of the dataset (see methods) is indicated
251 in the map captions.

252

253 **4.3 Analogue quality**

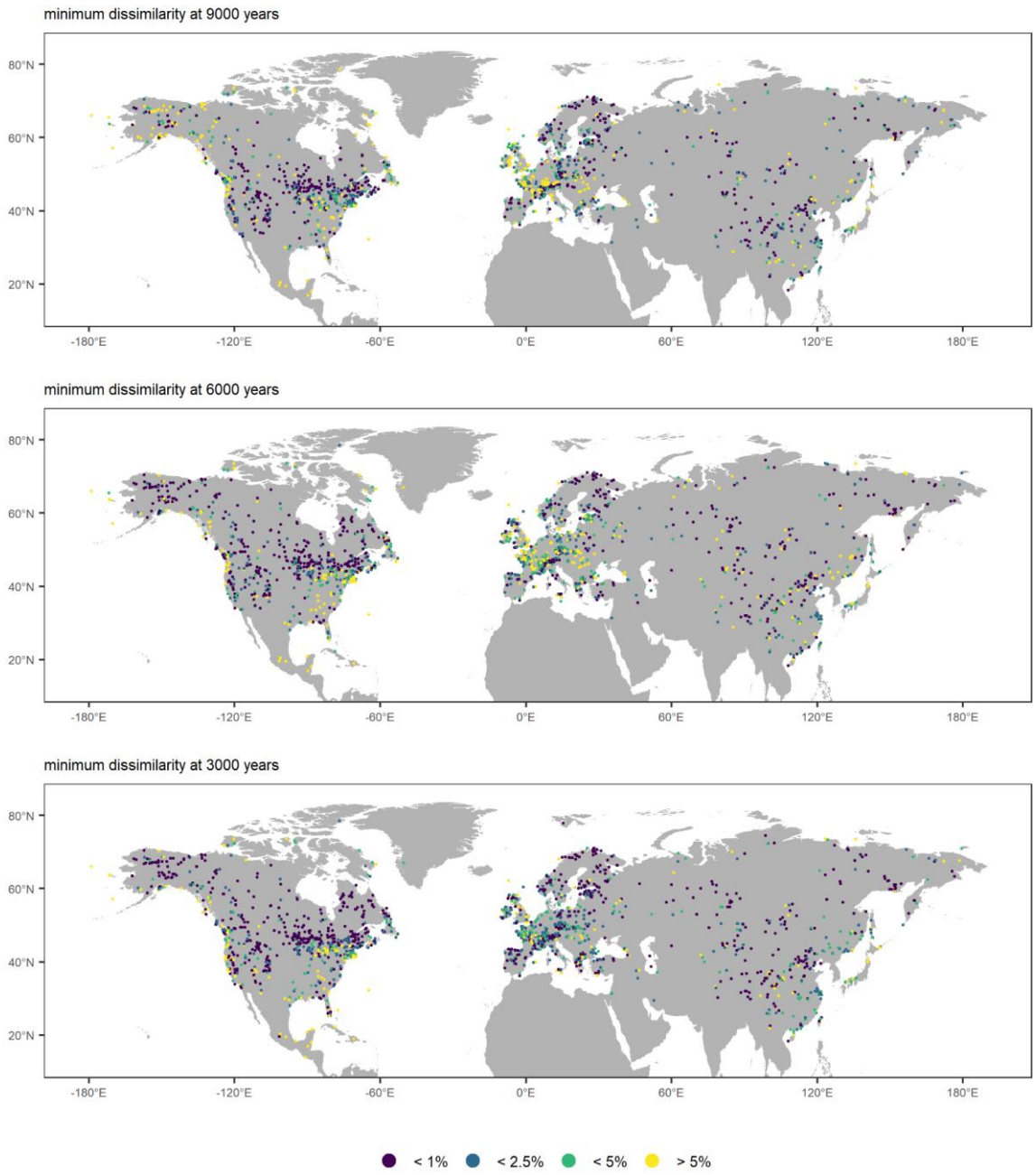

Figure 4. Analogue quality as assessed by squared chord distance between modern pollen assemblages and fossil pollen assemblages. Results identify a very good (<1%), good (<2.5%) and poor (<5%) analogues Distances >5% are considered to indicate non-analogue situations (as percentage of all distances among pollen samples in the modern dataset used for calibration).

The dissimilarity (squared chord distance) between modern pollen assemblages and fossil pollen assemblages was calculated and extracted for distinct time-slices at 9000, 6000 and 3000 years BP. In total, 36.4% (9000 years BP), 39.2% (6000 years BP) and 45.6% (3000 years BP) records indicate a

very good (<1%) analogue quality. The central part of the North American continent, Scandinavia and Central Asia show a very good analogue quality for all time-slices investigated. Poor (<5%) analogues can be found in Western Europe, the eastern parts of the United States and along the eastern Asian coastline. Non-analogues (>5%) are found for 22.6% (9000 years BP), 20.47% (6000 years BP) and 12.5% (3000 years BP) record respectively, especially in Western Europe and at 9000 years BP in Alaska.

4.4 Prediction errors of LegacyClimate 1.0

The mean RMSEPs and their standard deviations for T_{ann} are 1.98±0.52°C (MAT), 2.61±0.53°C (WA-PLS) and 2.24±0.61°C (WA-PLS_tailored) and mean RMSEPs as a percentage of modern T_{ann} range are 7.68±1.93% (MAT), 10.09±2.05% (WA-PLS) and 10.26±2.79% (WA-PLS_tailored). The largest mean RMSEP values are located in Central Asia in Kazakhstan, Mongolia and the north-western parts of the Tibetan Plateau and are consistent across all three reconstruction methods. Other areas with large mean RMSEP values are located in Western North America, Southern and Central Europe and south-east Asia. The smallest RMSEPs can be found along the east coast of North America. Relative to the modern temperature range, the RMSEP from this region also reveals the lowest fraction. In general, MAT has the lowest mean error fraction relative to the modern temperature range of all three methods.

The mean RMSEPs of T_{July} are 1.90±0.63°C (MAT), 2.50±0.73°C (WA-PLS) and 2.21±0.75°C (WA-PLS_tailored) and mean percentages of T_{July} range are 8.11±1.64% (MAT), 10.71±1.94% (WA-PLS) and 10.70±2.60% (WA-PLS_tailored). Thus, they are slightly smaller than those of T_{ann} but slightly larger as a percentage of the range. The spatial patterns, however, are largely similar to those of T_{ann}.

The mean RMSEPs of P_{ann} are 176.38±51.40 mm (MAT), 244.48±75.84 mm (WA-PLS) and 232.71±98.57 mm (WA-PLS_tailored) and mean percentages of P_{ann} range are 6.78±1.48% (MAT), 9.27±1.70% (WA-PLS) and 10.26±2.67% (WA-PLS_tailored). High RMSEPs are found for Western North America, Europe and along the coastline of south-east Asia, while the lowest RMSEP values are found for Central Asia. A clear division in RMSEPs are found on the North American continent: while the western part of North America (with the exception of Alaska) has a rather high RMSEP, the eastern part of North America has a smaller RMSEP. This pattern is found for all three methods (Fig. 5).

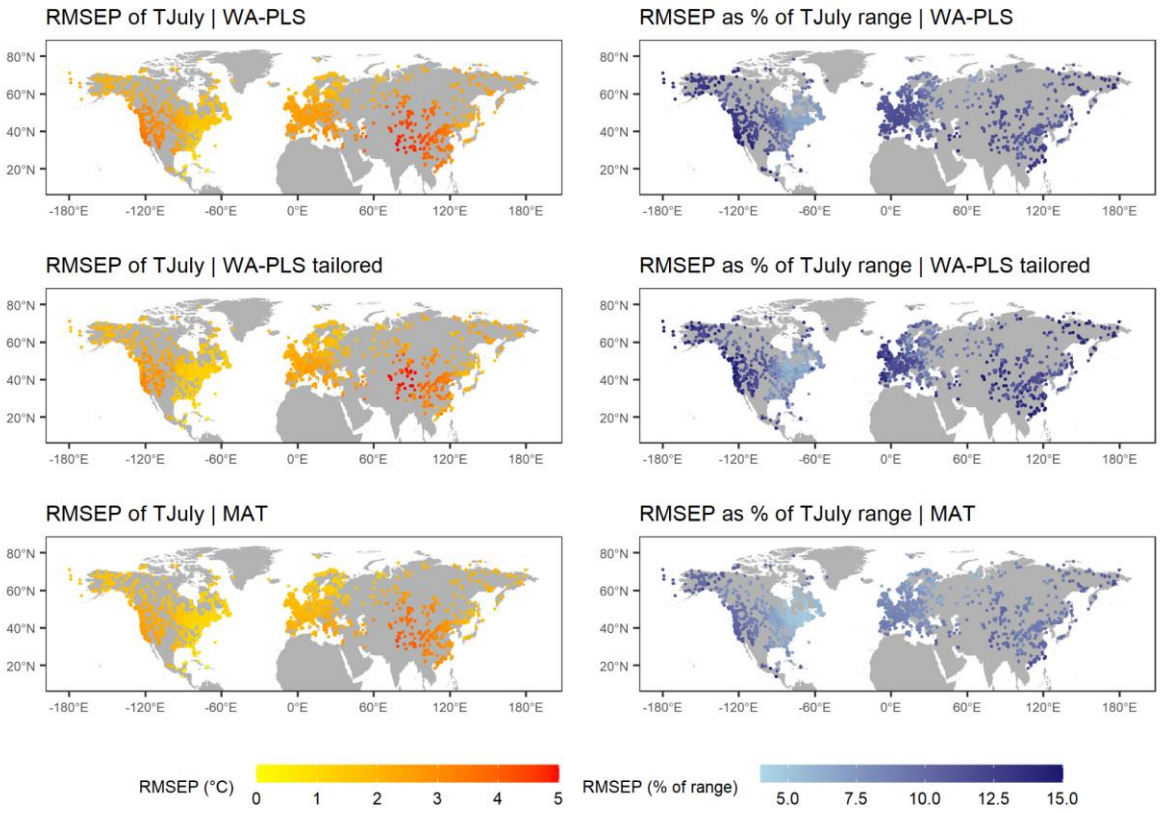
RMSEP of TJuly | WA-PLS
RMSEP as % of TJuly range | WA-PLS
RMSEP of TJuly | WA-PLS tailored
RMSEP as % of TJuly range | WA-PLS tailored
RMSEP of TJuly | MAT
RMSEP as % of TJuly range | MAT
80°N
60°N
40°N
20°N
-180°E
-120°E
-60°E
0°E
60°E
120°E
180°E
RMSEP (°C)
0 1 2 3 4 5
RMSEP (% of range)
5.0 7.5 10.0 12.5 15.0

293

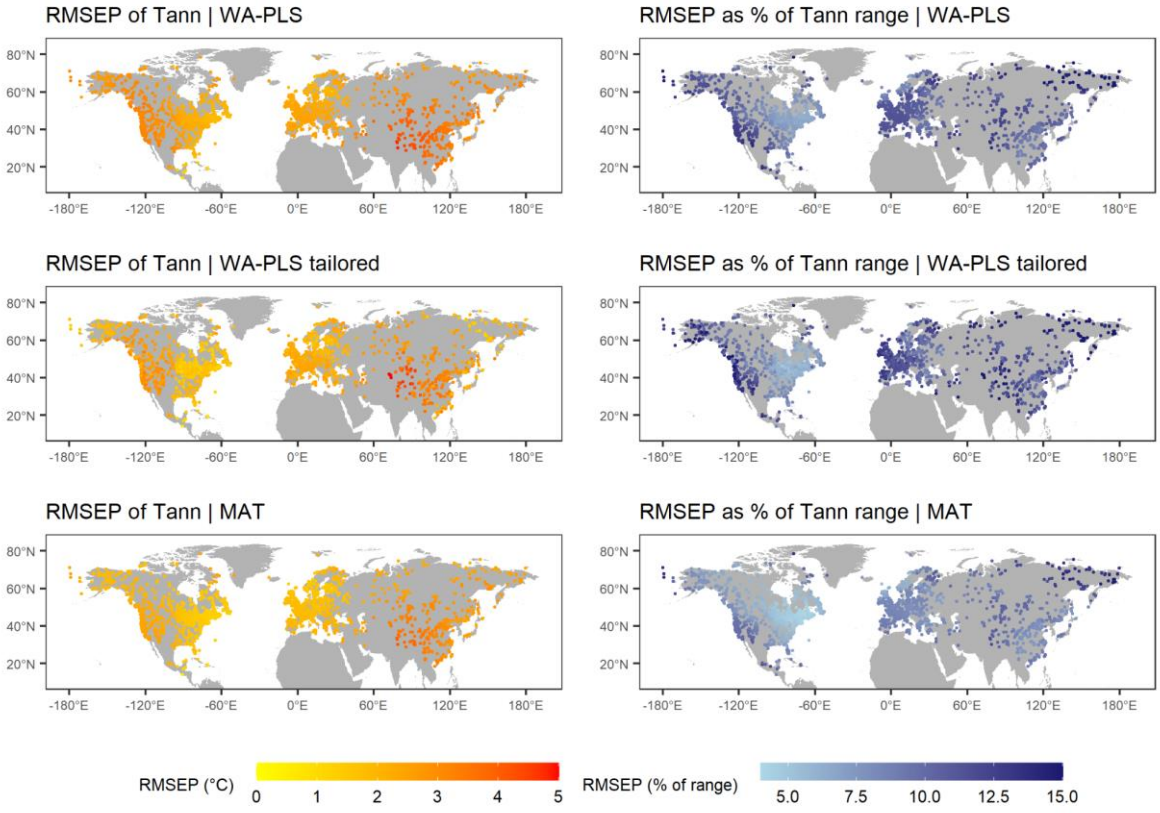
RMSEP of Tann | WA-PLS
RMSEP as % of Tann range | WA-PLS
RMSEP of Tann | WA-PLS tailored
RMSEP as % of Tann range | WA-PLS tailored
RMSEP of Tann | MAT
RMSEP as % of Tann range | MAT
80°N
60°N
40°N
20°N
-180°E
-120°E
-60°E
0°E
60°E
120°E
180°E
RMSEP (°C)
0 1 2 3 4 5
RMSEP (% of range)
5.0 7.5 10.0 12.5 15.0

294

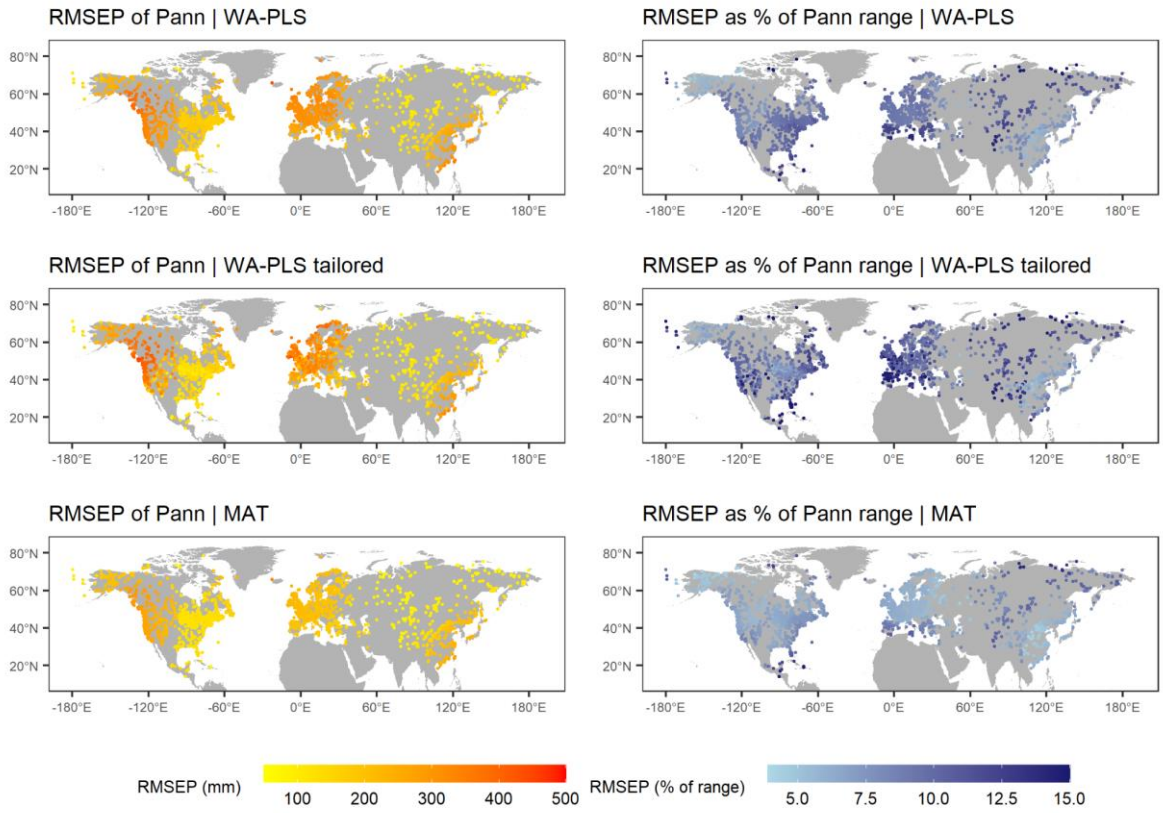

295

296 **Figure 5.** Spatial distribution of root-mean-squared error of prediction (RMSEP) as inferred from leave-
297 one-out cross-validation presented as absolute values and as a percentage of the range of mean July
298 temperature (T_{July}), mean annual temperature (T_{ann}), mean annual precipitation (P_{ann}) in the modern
299 pollen data used for reconstruction for the three methods applied (Weighted-Averaging Partial-Least
300 Squares regression (WA-PLS), WA-PLS using a training set from within a limited climate range (WA-
301 PLS_tailored) and Modern Analogue Technique (MAT)).

302

303 **4.5 Significance test**

304 A significance test ($p < 0.1$, see methods) according to Telford and Birks (2011) was performed for each
305 record (Fig. 6; Table 2). For the T_{July} reconstruction, 30.9% (WA-PLS) and 35.2% (WA-PLS_tailored) of
306 all records passed the significance test when included as a single variable in the significance test.
307 Partialling out precipitation as a conditional variable causes an increase in the amount of significant
308 records to 35.5% for WA-PLS of T_{July}, but a decrease for WA-PLS_tailored to 33.6% of all records. The
309 T_{ann} reconstruction is significant for 32.8% (WA-PLS) and 36.1% (WA-PLS_tailored) of all records when
310 tested as a single variable. When partialling out precipitation, the amount of significant records
311 decreases for both WA-PLS and WA-PLS_tailored. 32.1% (WA-PLS) and 33.4% (WA-PLS_tailored) of

all records pass the significance test when testing P_{ann} as a single variable. In contrast to the significance tests for T_{ann}, partialling out the mean July temperature as a conditional variable increases the number of significant records for both WA-PLS and WA-PLS_tailored.

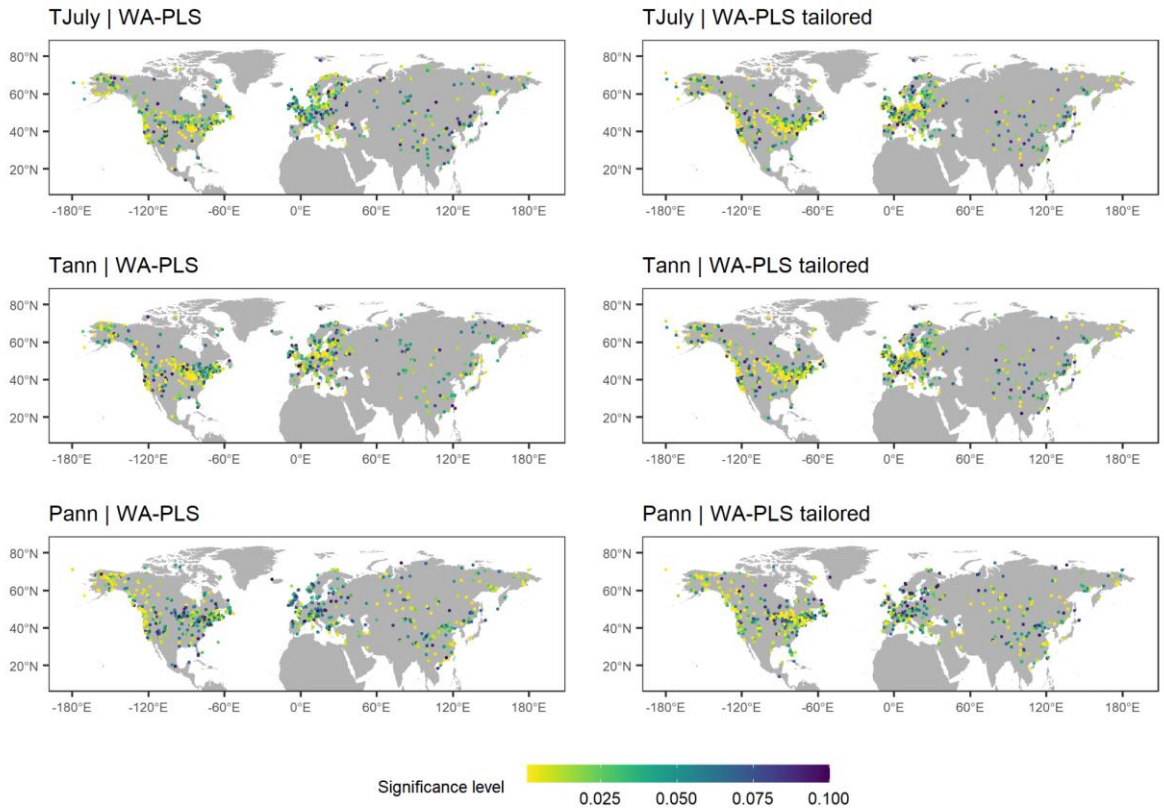

Figure 6. Maps showing mean July temperature (T_{July}), mean annual temperature (T_{ann}), mean annual precipitation (P_{ann}) records that passed the reconstruction significance test ($p<0.1$). Colors indicates the significance level.

Table 2. Percentage of records that pass the reconstruction significance test ($p<0.1$) sensu Telford and Birks (2011).

	WA-PLS	WA-PLS_tailored	MAT
T_{July}	30.9%	35.2%	
T_{July} partialling out P_{ann}	35.5%	33.6%	
T_{ann}	32.8%	36.1%	
T_{ann} partialling out P_{ann}	32.6%	34.1%	
P_{ann}	32.1%	33.4%	
P_{ann} partialling out T_{July}	34.3%	36.5%	

327

328 **4.6 Human impact**

329 We used the abundance of Plantaginaceae and *Rumex* as indicators of grazing and such intense animal
330 husbandry. Overall weak human impact is inferred for North America and Northern Asia. The indicators
331 indicate strong human impact only in single records at 9000 years BP in China and the Mediterranean
332 region (Fig. 7). The percentage values of Plantaginaceae and *Rumex* were high especially in Europe
333 for 3000 years and 1000 years BP which indicates growing human impact on that region. High
334 Plantaginaceae correlate with low T_{July} in Central Europe indicating potential biases in the temperature
335 reconstructions i.e. too low temperatures become reconstructed (Fig. 8).

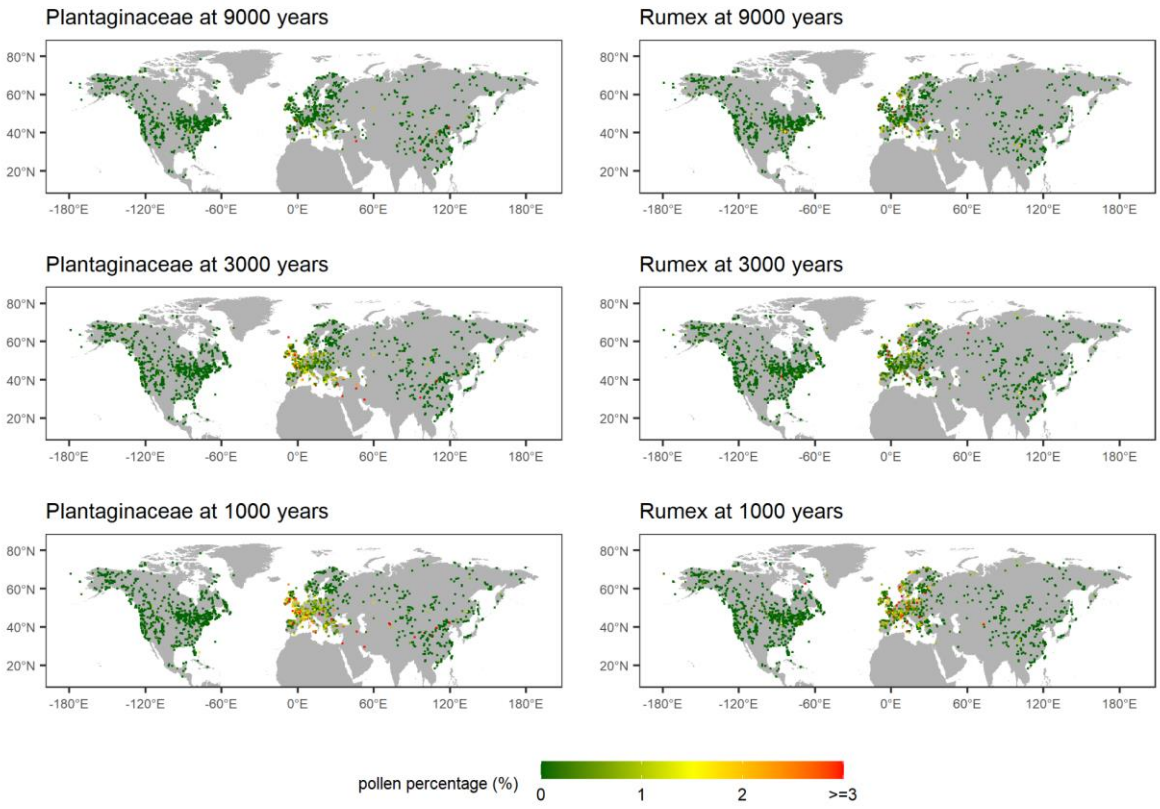

336

337 **Figure 7.** Abundance of Plantaginaceae (left) and *Rumex* (right) at 9000, 3000 and 1000 years BP.

338 Colors indicate percentage values.

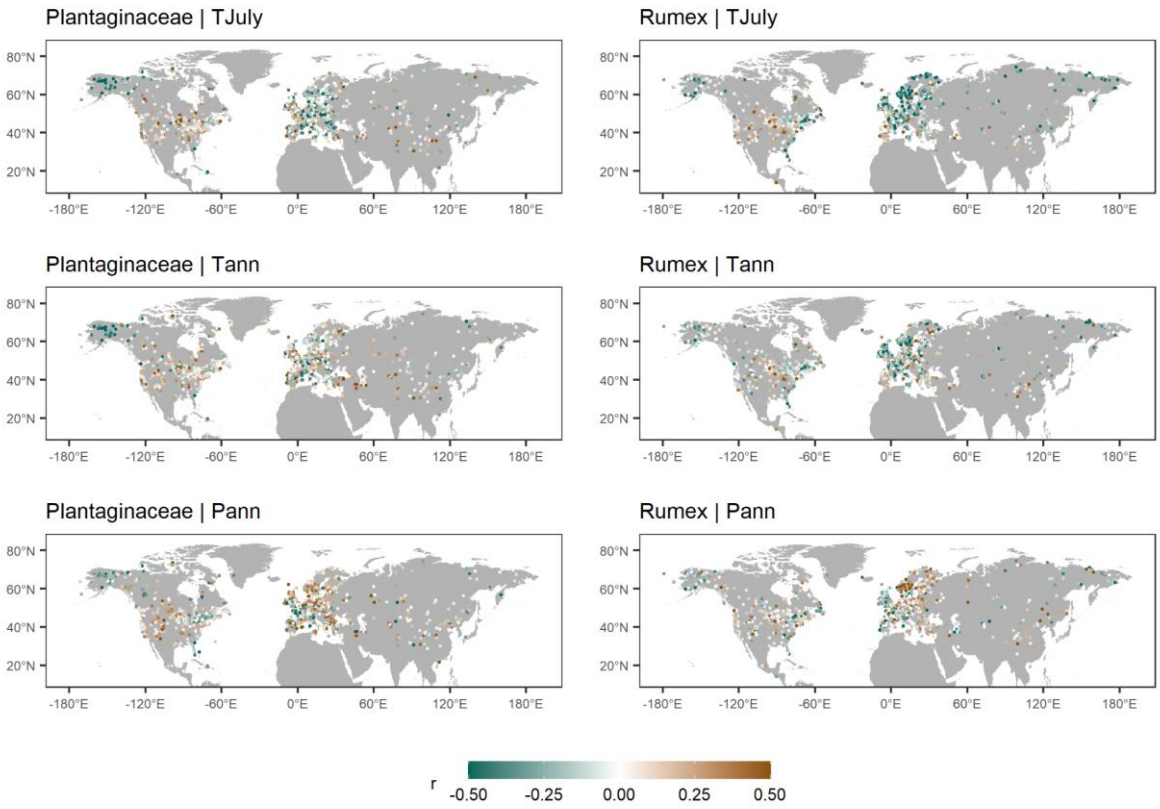

339

Figure 8. Correlation between the percentage of Plantaginaceae (left) and *Rumex* (right) and reconstructed T_{July}, T_{ann} and P_{ann} with WA-PLS.

4.7 Assessment of major temporal patterns of LegacyClimate 1.0

To illustrate the difference between Mid- and Late Holocene climate, we calculated the value for the three climate variables at 6 ka BP and 1 ka BP, each time taking the average of the interpolated values at those ages for the ensemble of 1000 realizations of the age-depth models (Li et al., 2022). Differences between these time-slices reveal warmer and drier conditions during Mid-Holocene compared with Late Holocene conditions, especially in Eastern North America but also in Central and Northern Europe. The overall patterns are in good agreement for all three methods but show differences on a regional scale, especially when comparing the reconstructions with WA-PLS and MAT. For T_{July}, the reconstruction with MAT shows greater temperature differences in Western North America and south-east Asia. Compared to the reconstruction with WA-PLS, there is a reduced cooling from 6 to 1 in Eastern Europe and a warming instead of a cooling in the Western Mediterranean region and along the south-eastern Asian coastline in MAT. For large areas in North America and Europe, the reconstructions with WA-PLS suggest an increase in precipitation from 6 to 1 ka BP. A shift to drier conditions can be found along the south-eastern coastline in North America, in the Mediterranean Region and especially in south-east Asia. The reconstruction with MAT reveals a gradient from increasing precipitation in south-western Europe to decreasing precipitation in north-eastern Europe. In contrast to the reconstructions with WA-PLS, records along the south-eastern Asian coastline suggest an increase in precipitation with MAT rather than a decrease (Fig. 9).

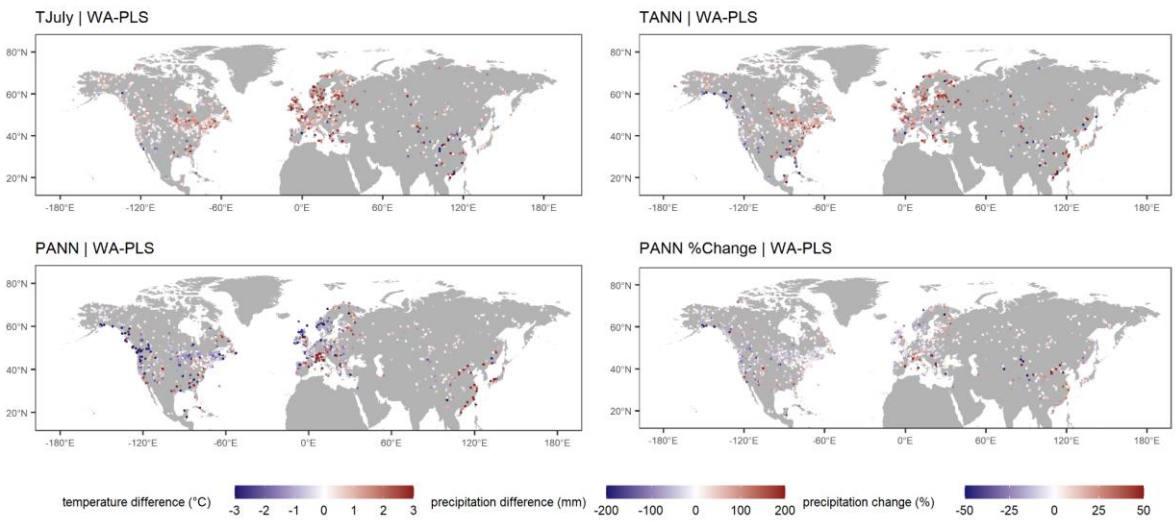

361

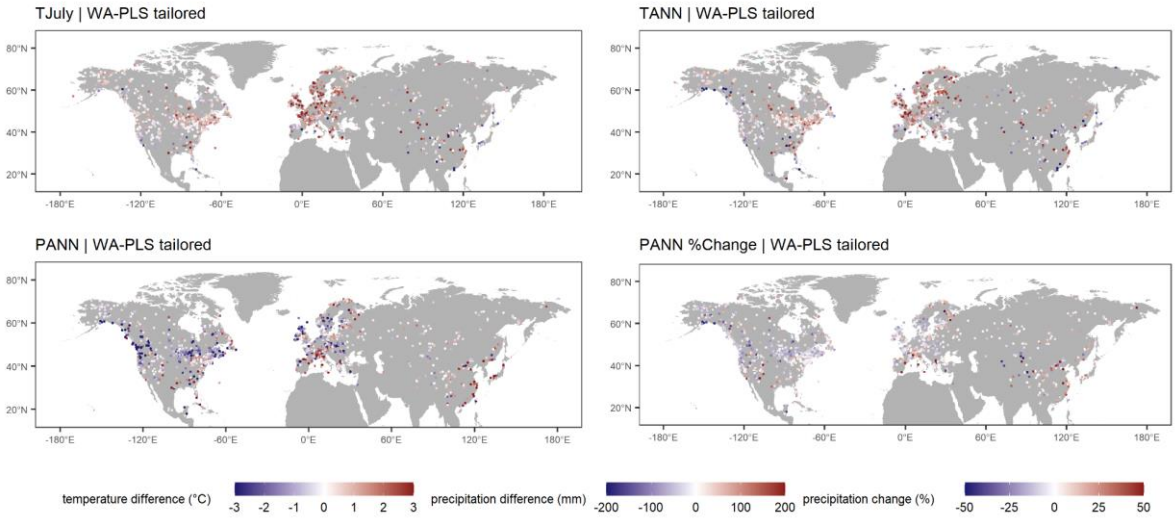

362

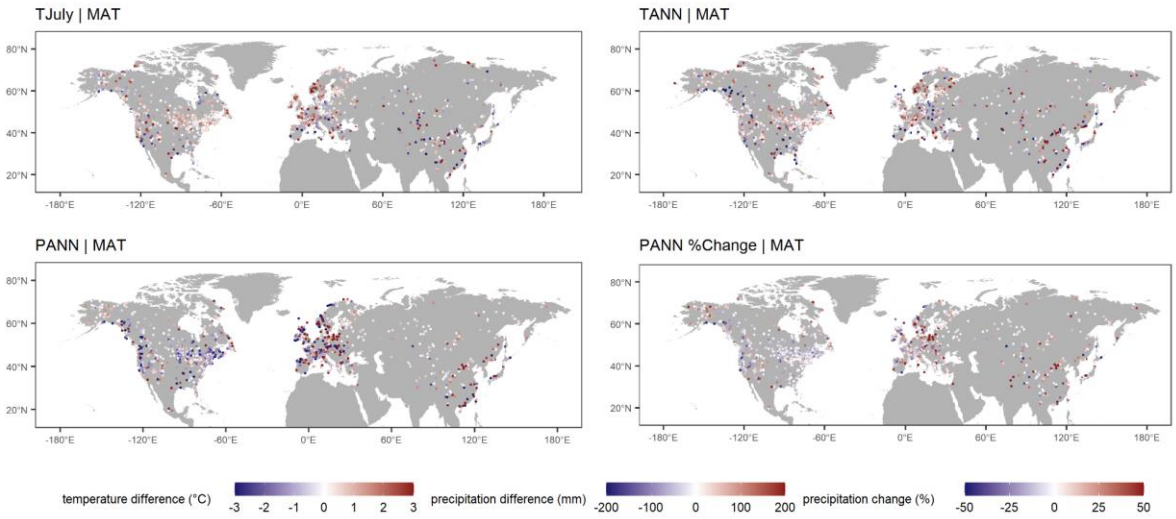

363

364 **Figure 9.** Difference from 6 ka to 1 ka for mean July temperature (T_{July}), mean annual temperature (T_{ann}),
365 mean annual precipitation (P_{ann}) and P_{ann}% as reconstructed from WA-PLS (upper panel), WA-
366 PLS_tailored (middle panel) and MAT (lower panel).

Time-series of absolute T_{ann} reconstructions reveal temporal as well as latitudinal spatial variation on the single continents. Eastern North America and Asia show the most variation in the low latitudes. It is also Eastern North America which shows the most pronounced latitudinal gradient. In Western North America, the most variation takes place in the high latitudes, while the variation is concentrated to the mid-latitudes in Europe. Especially in North America, the warming since the last deglaciation and the beginning of the Holocene is well shown in the temporal variation of the time-series (Fig. 10).

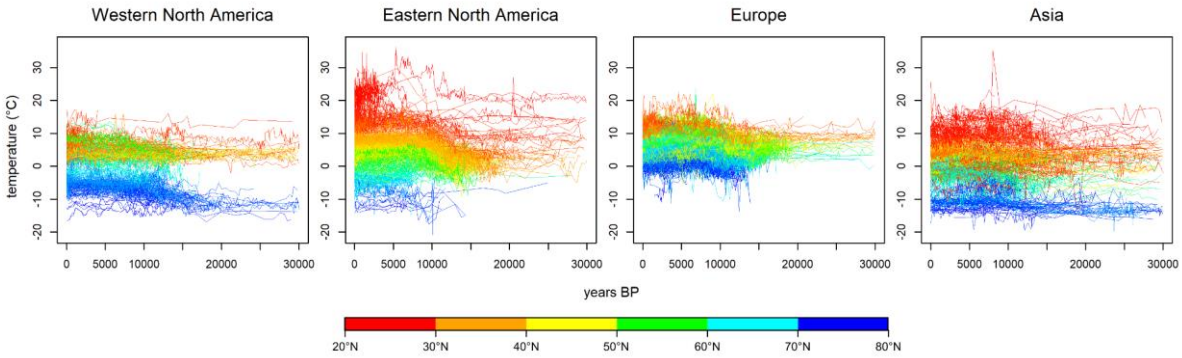

Figure 10. Time-series of absolute mean annual temperature (T_{ann}) reconstruction for each (sub-)continent. Colors denote the latitude of record origin. Age and reconstruction uncertainties are not plotted but are available for each time-series.

4.8 Assessment of consistency among reconstruction methods

Reconstructions with MAT are, in general, in good agreement with those derived from the WA-PLS. Comparing MAT with WA-PLS, 37.3% (T_{July}), 38.9% (T_{ann}) and 30.4% (P_{ann}) of all records have a positive correlation of r >= 0.6. Strong positive correlations (r >= 0.9) can mainly be identified in Eastern North America, while weak correlation can be found for large areas in central North America and most of Europe (Fig. 11).

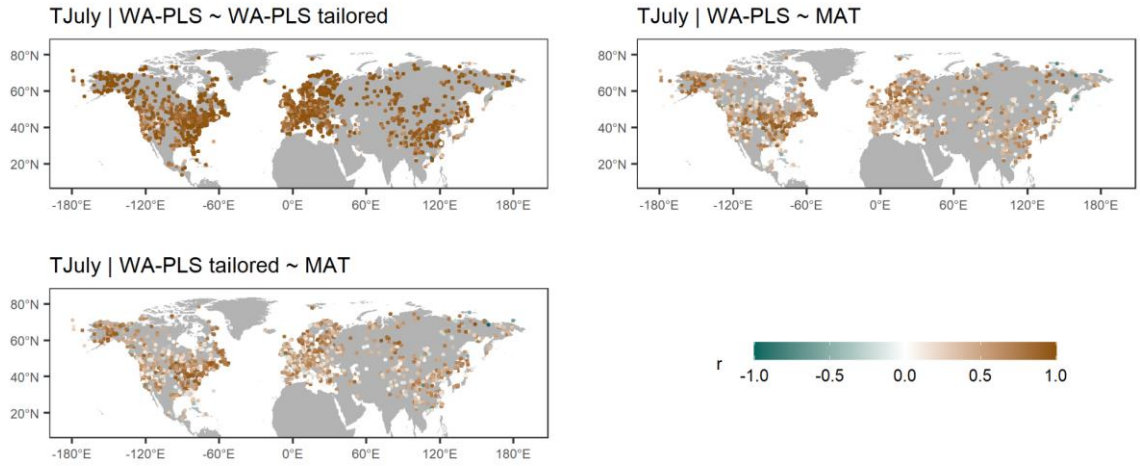

385

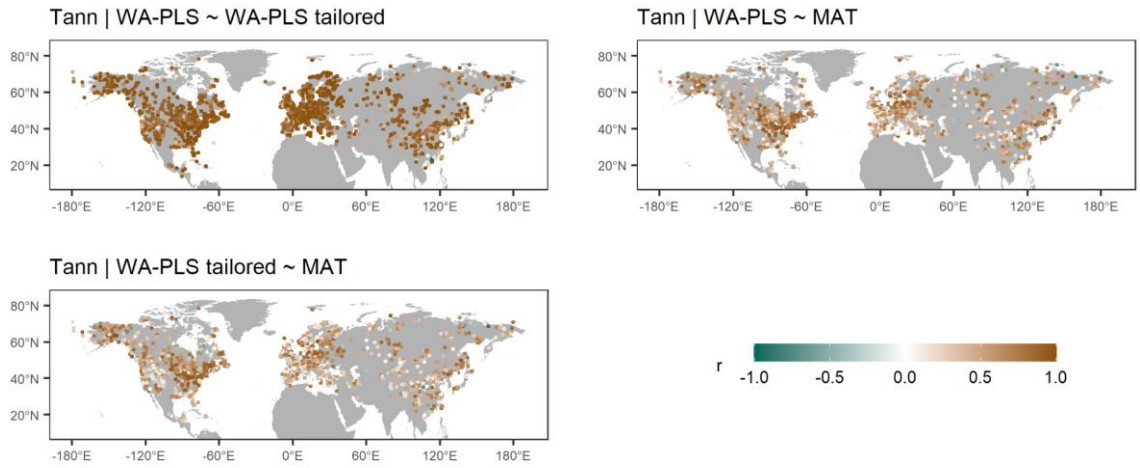

386

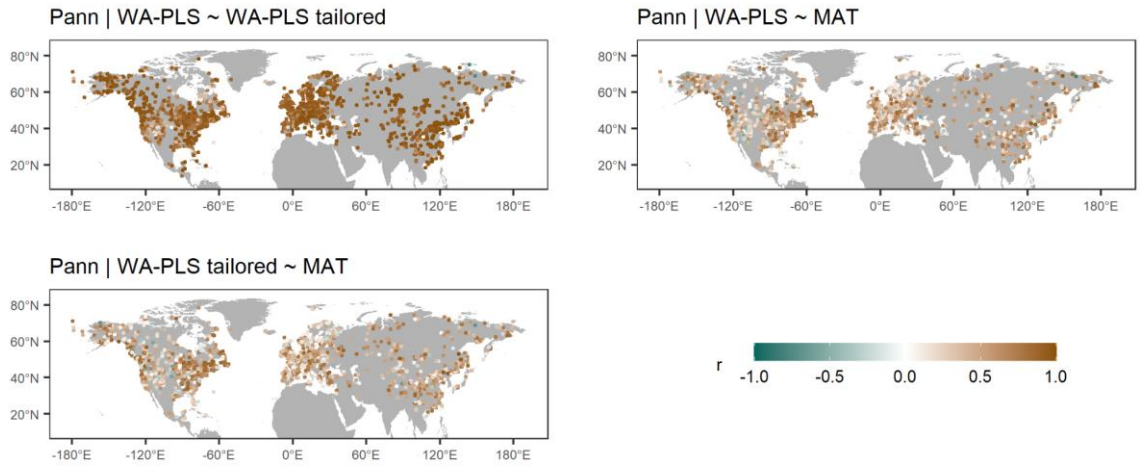

387

388 **Figure 11.** Correlation between time-series of the 3 different reconstruction methods used - weighted-
389 averaging partial least squares using a global training set (WA-PLS), WA-PLS using a training set with
390 a limited modern climate range (WA-PLS_tailored) and the modern analogue technique (MAT) for the

three climate variables of mean July temperature (T_{July}), mean annual temperature (T_{ann}) and mean annual precipitation (P_{ann})

WA-PLS_tailored used a reduced modern training dataset (illustrated for an example in Appendix Fig. 1). The tailoring successfully reduced the co-variation of temperature and precipitation in the modern dataset as indicated by the distribution of the correlation coefficient in Fig. 12. Nevertheless, the obtained reconstructions are largely consistent between WA-PLS and WA-PLS-tailored: a correlation of r >= 0.9 is found for 59.2% of all records for T_{July}, 60.7% for T_{ann} and 56.5% for P_{ann}.

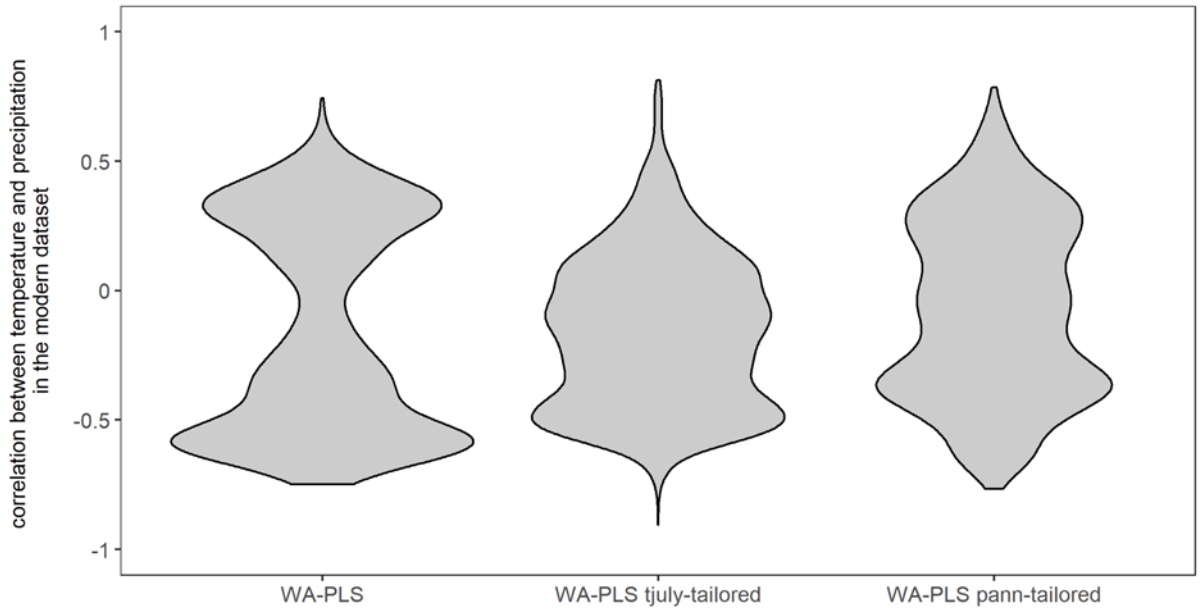

Figure 12. Violin plot of the correlation coefficients between T_{July} and P_{ann} in the 15379 training datasets used for the reconstructions. Left: used for WA-PLS reconstructions; middle: WA-PLS T_{July}-tailored (used for the reconstruction of P_{ann}); WA-PLS P_{ann}-tailored (used for the reconstruction of T_{July}).

5 Discussion

5.1 Impact of the fossil pollen data source on LegacyClimate 1.0 quality

LegacyClimate 1.0 contains reconstructions of climate variables from fossil pollen data derived from open-access data repositories. The fossil records were derived from multiple natural archives, most commonly, assemblages from continuous lacustrine and peat accumulations (Herzschuh et al., 2022c). Different sizes of lakes and peat areas result in varying sizes of pollen source areas and thus the spatial representativeness of a record, while small lakes and peatlands are considered to provide information

about the (extra-)local scale, while the regional signal is better represented in pollen assemblages from large lakes (Jackson, 1990; Sugita, 1993). However, taphonomic changes of the records originating, for example, from lake level changes may impact the reconstructed climate pollen from azonal riverine vegetation might be over-represented in fluvially impacted pollen records.

Our dataset is based on taxonomically harmonized modern and fossil pollen datasets using a restricted number of taxa. Such an approach guarantees that all records are handled consistently. Although losing taxonomic information when merging taxa together into a higher taxonomic level, it also increases the possibility of matching climate analogues in the modern and the fossil datasets. However, one needs to keep in mind that species with different ecological requirements may be merged together into one genus or family, for example, *Pinus* species that are restricted to tropical or subtropical areas in China or ones that grow in boreal forests (Cao et al., 2013; Tian et al., 2017).

Along with the pollen assemblages, data repositories also provide chronological information for fossil records. The quality of such chronologies varies strongly with respect to dating methods, calibration and numerical algorithms for determining an age-depth relationship (Blois et al., 2011; Trachsel and Telford, 2017). Having accurate and precise chronologies is thus of pivotal importance for reconstructing past climate in order to identify temporo-spatial patterns and therefore in helping to evaluate climate model outputs. The advantage of the fossil pollen dataset used for the reconstruction presented here (i.e., LegacyPollen 1.0; Herzschuh et al., 2022c) is that it has harmonized chronologies (LegacyAge 1.0) along with information about uncertainties as well as related metadata and scripts that allow a customized re-establishment of the chronologies (Li et al., 2022). Accordingly, we were able to provide sample specific age-uncertainties along with reconstruction uncertainties.

5.2 Modern pollen and climate data sources and LegacyClimate 1.0 quality

For our study we used the, to our knowledge, largest modern dataset ever used in a pollen-based climate reconstruction. For fossil pollen records in areas with an insufficient coverage of modern surface pollen samples (e.g., Central Asia or Western Siberia), it might be difficult to create a calibration dataset that maps the required variety of environmental and climatic gradients and therefore find enough modern analogues for reconstructions with a classification approach such as MAT. This is indicated by the high RMSEPs as percentages of gradient length in these areas. Our routine uses the modern pollen data

from within a radius of 2000 km around the site of the fossil record. The information provided in the reconstruction metadata including number of modern pollen samples and ranges of reconstructed variables, allows an assessment of the modern dataset used for reconstruction.

We a priori selected T_{July}, T_{ann} and P_{ann} as target variables for our reconstructions. However, we provide λ_1/λ_2 (i.e. explained variance of the climate variable in the modern pollen data set relative to the variance explained by the unconstrained first axis; ter Braak, 1988), a commonly used proxy for the assessment of reconstructions. The higher λ_1/λ_2 in the spatial modern dataset the higher the chance that this target climate variable has also impacted vegetation over time and is thus reflected in the variation of the fossil pollen dataset. As a rule of thumb, a ratio of 1 is considered to indicate reliable reconstructions (Juggins, 2012) though useful reconstruction may also be obtained from datasets with lower values. As expected, maps of RMSEPs reveal similar spatial pattern as the results of constrained ordination. Our results indicate that in particular calibration sets from Europe have low ratios and a high RMSEP for all climate variables (despite we have a high number of modern samples), likely related to the human impact on the modern and fossil data. Some areas that are known for its sensitivity to precipitation e.g. Eastern Asia show low RMSEPs as expected for P_{ann} but on the other hand show a low sensitivity to T_{ann} and T_{July}.

5.3 Reconstruction method and LegacyClimate 1.0 quality

Overall, the three reconstruction approaches, MAT, WA-PLS and WA-PLS_tailored yield rather similar results i.e. indicated by the overall high correlation between the reconstructions of the different methods (Fig. 11). Accordingly, the major trends at global or continental scales are similar, even if the actual amplitude of change may vary locally. As each method has its own strengths and weaknesses, there is not one set of reconstructions that is absolutely superior. One advantage of our multi-method reconstruction dataset is that users can identify the methods that are likely to perform best in a selected region and/or specific reconstructions. MAT is often recommended for large-scale studies, but it is highly sensitive to the quality of analogues (Chevalier et al. 2020). Low analogue situations can arise from two causes: climate conditions that differ strongly from today (e.g., the low atmospheric CO_2 concentration during the LGM; Jackson and Williams, 2004), or in regions with limited modern samples (e.g., extratropical Asia). We report the analogue distance for each sample to help identify such situations.

From our assessments, we revealed that analogues quality is overall rather good at least for the Holocene and except for Western Europe in particularly the British Isles (Fig. 4).

In contrast MAT, WA-PLS (and most regression techniques in general) model relationships between pollen and climate and are, as such, less sensitive to the low analogue situations (Birks et al., 2010). They are, however, based on some modelling assumptions, such as the unimodality of the response of the pollen taxa to climate (ter Braak and Juggins 1993). This condition is not always met at the continental scale, primarily because of the limited taxonomic resolution of pollen data that merges several plant species with distinct climate requirements as one single pollen taxon. WA-PLS_tailoring has the same limitation but it has the advantage of reducing the influence of the correlation between variables when reconstructing, for instance, temperature and precipitation. This may be particularly relevant for regions with a temperature-moisture driven circulation system such as the East Asian Summer Monsoon (EASM) that can heavily affect precipitation patterns in certain regions (Herzschuh et al., 2019). Using WAPLS_tailoring also increases the number of records that pass a significance level of $p < 0.1$ (Telford and Birks, 2011). Providing several reconstructions based on different assumptions also allow exploring, even if only partially, the uncertainties associated with the modelling assumptions (e.g., MAT vs WA-PLS, the number of analogues, type metric used to compare pollen samples).

All reconstruction methods used in this study heavily rely on extensive collections of modern assemblage data covering diverse climatic and environmental gradients and are applicable on a broad spatial scale. As discussed, all the methods may struggle with some intrinsic characteristics of pollen data and of pollen compilations, including complex species responses, sensitivity to spatial autocorrelation, limited analogues that may produce poor results in so-called “quantification deserts” (Chevalier, 2019), where fossil pollen is hardly preserved or nearby modern surface pollen samples are missing (Chevalier et al., 2020). However, we designed our datasets so that more methods can be included in our reconstruction scripts (https://doi.org/10.5281/zenodo.5910989; Herzschuh et al., 2022b), such as CREST, an approach that combines presence-only occurrence data from species distribution databases instead of modern pollen samples to estimate the responses of pollen taxa to the climate variable to reconstruct to a climate variable (Chevalier et al., 2014 and 2022). CREST is, therefore, more independent from the availability of modern pollen samples. Employing the Inverse-Modelling through iterative forward modeling (IMIFM) (Izumi and Bartlein, 2016) might also be possible in such regions. Its use would be particularly interesting to reconstruct the LGM samples, because IMIFM is the only technique that can explicitly take the effect of CO_2 on plants (Chevalier et al., 2020). The inclusion of

499 CREST and/or IMIFM in such large scale studies would complement our multi-model reconstruction
500 ensemble by exploring a larger fraction of the “method uncertainty” space in greater details (e.g. Brewer
501 et al, 2008).

502

503 **5.4 Potential use of LegacyClimate 1.0**

504 Our LegacyPollen 1.0 fossil pollen synthesis (Herzschuh et al., 2022c) contains records from all over
505 the Northern Hemisphere extratropics. Climate reconstruction data sets like LegacyClimate 1.0 thus can
506 be used to infer spatio-temporal patterns in climate reconstructions that are not only limited to a local or
507 regional scale. Although several hemispheric or global reconstruction studies exist, they have been
508 largely restricted to temperature or have included relatively few records (Marcott et al., 2013; Marsicek
509 et al., 2018; Routson et al., 2019; Kaufman et al., 2020a and 2020b). Our dataset is therefore a valuable
510 addition. It may be used in a multi-proxy approach, synthesizing marine and terrestrial records in order
511 to assess temperature development during the Holocene and can help to highlight possible
512 interdependencies between oceans and land masses and such contribute to the “Holocene conundrum”
513 debate (Liu et al., 2014). Temperature reconstructions from proxy data indicate peak temperatures
514 during the Holocene Thermal Maximum around 6000 years BP followed by a pronounced cooling trend
515 toward the late Holocene (Kaufman et al., 2020b), which is also visible in our pollen-based
516 reconstructions (Fig. 6). In contrast, climate models simulate a monotonic warming throughout the
517 Holocene, which resulted in the “Holocene conundrum” debate (Liu et al., 2014). Temperature
518 reconstructions are often derived from sea-surface temperatures as either mean annual temperatures
519 (Birks, 2019; Bova et al., 2021) or global mean surface temperature (Marcott et al., 2013; Marsicek et
520 al., 2018; Kaufman et al., 2020a and 2020b). However, it is argued that proxy-based climate
521 reconstructions are seasonally biased and therefore might be the reason for the observed proxy-model
522 divergence (Liu et al., 2014; Rehfeld et al., 2016; Kaufman et al., 2020b). In this respect, it might help
523 that we provide T_{July} along with T_{ann} reconstructions derived from our tailoring approach, which provides
524 the opportunity to assess seasonal impacts on the reconstruction.

525 So far, reconstructions of precipitation have not been implemented on a hemispheric scale. The
526 interconnection between temperature and precipitation (Trenberth, 2011) and its spatio-temporal
527 variation across the Northern Hemisphere is therefore an important aspect of evaluating climate models

(Wu et al., 2013; Hao et al., 2019; Herzschuh et al., 2022a). A broad-scale quantitative reconstruction of temperature and precipitation would therefore be of great value for evaluating transient climate model experiments such as TraCE 21k (He, 2010).

Our assessments of the modern dataset (e.g. using CCA), the transfer function (e.g. RMSEP) and the reconstruction (e.g. the significance test) revealed also the potential biases in the pollen-based reconstruction and pointed to limitations. Further validation and assessments of the results and more comprehensive uncertainty analyses e.g. by applying forward modelling approaches (Izumi & Bartlein, 2016; Parnell et al., 2016) would be highly valuable.

6 Data and code availability

The compilation of reconstructed T_{July}, T_{ann}, and P_{ann}, is open access and available at PANGAEA (https://doi.pangaea.de/10.1594/PANGAEA.930512; in the "*Other version*" section; Herzschuh et al., 2021). The dataset files are stored in machine-readable data format (.CSV), which are already separated into Western North America, Eastern North America, Europe, and Asia for easy access and use.

The R code to run the reconstructions for single sites is available at Zenodo (https://doi.org/10.5281/zenodo.5910989; Herzschuh et al., 2022b) including harmonized open-access modern and fossil pollen datasets so that customized reconstructions can be easily established.

Appendix Figures

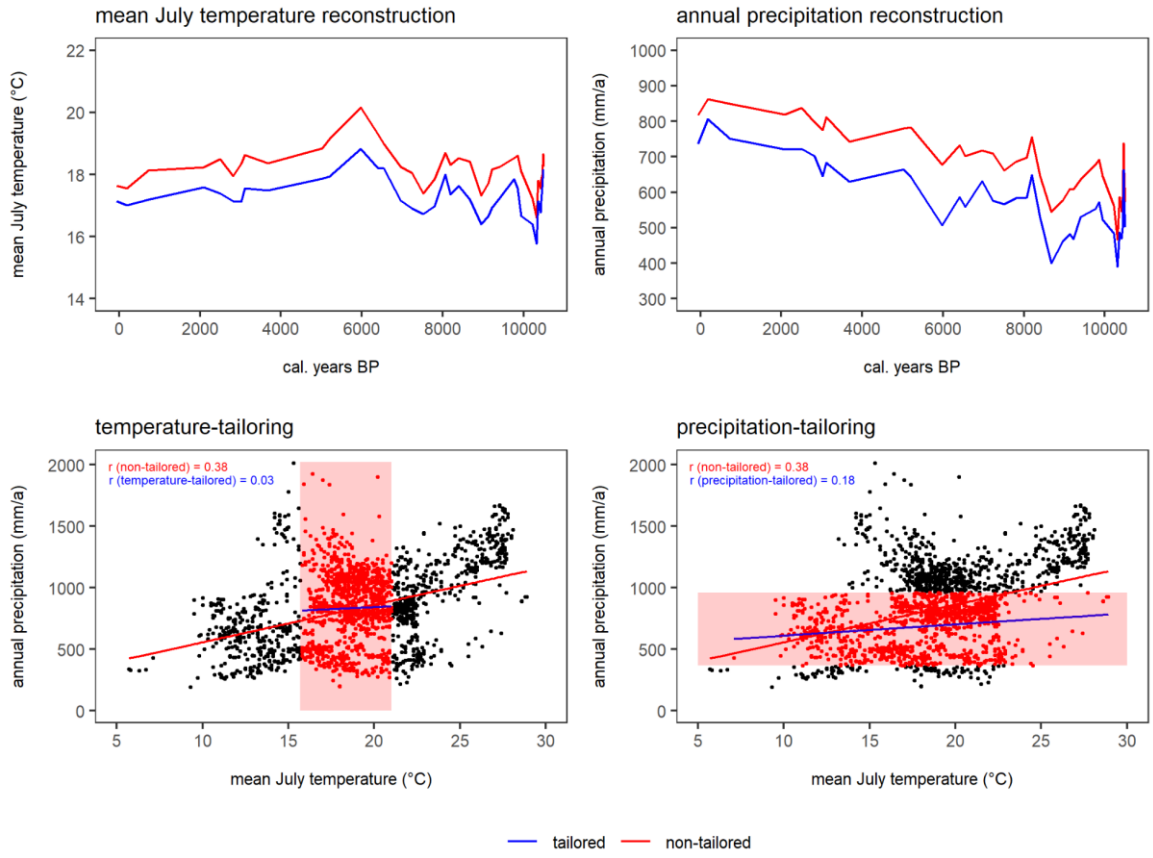

Appendix Figure 1. Example to illustrate the effect of tailoring the modern dataset for the location "Yellow Dog Pond" in Eastern North America. Upper part: reconstruction of T_{July} and P_{ann} with WA-PLS (red) and WA-PLS_tailored (blue); lower part: correlation of T_{July} and P_{ann} in the modern dataset and the effect of tailoring the modern dataset (indicated with the red box). Correlations are given for non-tailored (red) and tailored (blue) data.

Author contributions. UH designed the study design and reconstruction dataset. CL and TB compiled the metadata and the harmonized pollen dataset. TB wrote the R scripts and ran the analyses under the supervision of UH. UH, TB and MC wrote the first draft of the manuscript. All authors discussed the results and contributed to the final manuscript.

Competing interests. The contact author has declared that none of the authors has any competing interests.

Acknowledgements. We would like to express our gratitude to all the palynologists and geologists who, either directly or indirectly by providing their work the Neotoma Paleoecology Database, contributed pollen data and chronologies to the dataset. The work of data contributors, data stewards, and the Neotoma community is gratefully acknowledged. We thank Andrej Andreev, Mareike Wieczorek, and Birgit Heim from AWI for providing information on pollen records and data uploads. We also thank Cathy Jenks for language editing on a previous version of the paper.

Financial support. This research has been supported by the European Research Council (ERC Glacial Legacy 772852 to UH) and the PalMod Initiative (01LP1510C to UH). TB and MC is supported by the German Federal Ministry of Education and Research (BMBF) as a Research for Sustainability initiative (FONA; https://www.fona.de/en) through the PalMod Phase II project (grant no. FKZ: 01LP1926D). CL holds a scholarship from the Chinese Scholarship Council (grant no. 201908130165). NR work was supported by the Russian Science Foundation (Grant No. 20-17-00110).

References

Behre, K. E.: The rôle of man in European vegetation history. In: Huntley, B., Webb, T. (eds) Vegetation history. Handbook of vegetation science, vol 7. Springer, Dordrecht. https://doi.org/10.1007/978-94-009-3081-0_17, 1988.

Birks, H. J. B.: Contributions of Quaternary botany to modern ecology and biogeography, Plant Ecol. Divers., 12, 189–385, https://doi.org/10.1080/17550874.2019.1646831, 2019.

Birks, H. J. B., Heiri, O., Seppä, H., and Bjune, A. E.: Strengths and Weaknesses of Quantitative Climate Reconstructions Based on Late-Quaternary, Open Ecol. J., 3, 68–110, http://dx.doi.org/10.2174/1874213001003020068, 2010.

Blaauw, M. and Christen, J. A.: Flexible paleoclimate age-depth models using an autoregressive gamma process, Bayesian Anal., 6, 457–474, https://doi.org/10.1214/11-BA618, 2011.

Blois, J. L., Williams, J. W., Grimm, E. C., Jackson, S. T., and Graham, R. W.: A methodological framework for assessing and reducing temporal uncertainty in paleovegetation mapping from late-

Quaternary pollen records, Quat. Sci. Rev., 30, 1926–1939, https://doi.org/10.1016/j.quascirev.2011.04.017, 2011.

Bova, S., Rosenthal, Y., Liu, Z., Godad, S. P., and Yan, M.: Seasonal origin of the thermal maxima at the Holocene and the last interglacial, Nature, 589, 548–553, https://doi.org/10.1038/s41586-020-03155-x, 2021.

Brewer, S., Guiot, J., Sánchez-Goñi, M. F., and Klotz, S.: The climate in Europe during the Eemian: a multi-method approach using pollen data, Quaternary Science Reviews, 27, 2303–2315, https://doi.org/10.1016/j.quascirev.2008.08.029, 2008.

Cao, X., Ni, J., Herzschuh, U., Wang, Y., and Zhao, Y.: A late Quaternary pollen dataset from eastern continental Asia for vegetation and climate reconstructions: Set up and evaluation, Rev. Palaeobot. Palynol., 194, 21–37, https://doi.org/10.1016/j.revpalbo.2013.02.003, 2013.

Cao, X., Herzschuh, U., Telford, R. J., and Ni, J.: A modern pollen–climate dataset from China and Mongolia: Assessing its potential for climate reconstruction, Rev. Palaeobot. Palynol., 211, 87–96, https://doi.org/10.1016/j.revpalbo.2014.08.007, 2014.

Cao, X., Tian, F., Telford, R. J., Ni, J., Xu, Q., Chen, F., Liu, X., Stebich, M., Zhao, Y., Herzschuh, U.,: Impacts of the spatial extent of pollen-climate calibration-set on the absolute values, range and trends of reconstructed Holocene precipitation. Quaternary Science Reviews 178, 37-53. https://doi.org/10.1016/j.quascirev.2017.10.030, 2017.

Cao, X., Tian, F., Andreev, A., Anderson, P. M., Lozhkin, A. V., Bezrukova, E., Ni, J., Rudaya, N., Stobbe, A., Wieczorek, M., and Herzschuh, U.: A taxonomically harmonized and temporally standardized fossil pollen dataset from Siberia covering the last 40 kyr, Earth Syst. Sci. Data, 12, 119–135, https://doi.org/10.5194/essd-12-119-2020, 2020.

Chen, F., Chen, J., Huang, W., Chen, S., Huang, X., Jin, L., Jia, J., Zhang, X., An, C., Zhang, J., Zhao, Y., Yu, Z., Zhang, R., Liu, J., Zhou, A., and Feng, S.: Westerlies Asia and monsoonal Asia: Spatiotemporal differences in climate change and possible mechanisms on decadal to sub-orbital timescales, Earth Sci. Rev., 192, 337–354, https://doi.org/10.1016/j.earscirev.2019.03.005, 2019.

620 Chevalier, M.: Enabling possibilities to quantify past climate from fossil assemblages at a global scale,
621 Glob. Planet. Change, 175, 27–35, https://doi.org/10.1016/j.gloplacha.2019.01.016, 2019.

622 Chevalier, M.: *crestr*: an R package to perform probabilistic climate reconstructions from
623 palaeoecological datasets, Clim. Past, 18, 821–844, https://doi.org/10.5194/cp-18-821-2022, 2022.

624 Chevalier, M., Cheddadi, R., and Chase, B. M.: CREST (Climate REconstruction SofTware): a
625 probability density function (PDF)-based quantitative climate reconstruction method, Clim. Past, 10,
626 2081–2098, https://doi.org/10.5194/cp-10-2081-2014, 2014.

627 Chevalier, M., Davis, B. A. S., Heiri, O., Seppä, H., Chase, B. M., Gajewski, K., Lacourse, T., Telford,
628 R. J., Finsinger, W., Guiot, J., Kühl, N., Maezumi, S. Y., Tipton, J. R., Carter, V. A., Brussel, T.,
629 Phelps, L. N., Dawson, A., Zanon, M., Vallé, F., Nolan, C., Mauri, A., de Vernal, A., Izumi, K.,
630 Holmström, L., Marsicek, J., Goring, S., Sommer, P. S., Chaput, M., and Kupriyanov, D.: Pollen-
631 based climate reconstruction techniques for late Quaternary studies, Earth Sci. Rev., 210, 103384,
632 https://doi.org/10.1016/j.earscirev.2020.103384, 2020.

633 Davis, B. A. S., Zanon, M., Collins, P., Mauri, A., Bakker, J., Barboni, D., Barthelmes, A., Beaudouin,
634 C., Bjune, A. E., Bozilova, E., Bradshaw, R. H. W., Brayshay, B. A., Brewer, S., Brugiapaglia, E.,
635 Bunting, J., Connor, S. E., de Beaulieu, J.-L., Edwards, K., Ejarque, A., Fall, P., Florenzano, A.,
636 Fyfe, R., Galop, D., Giardini, M., Giesecke, T., Grant, M. J., Guiot, J., Jahns, S., Jankovská, V.,
637 Juggins, S., Kahrmann, M., Karpińska-Kołaczek, M., Kołaczek, P., Kühl, N., Kuneš, P., Lapteva, E.
638 G., Leroy, S. A. G., Leydet, M., Guiot, J., Jahns, S., Jankovská, V., Juggins, S., Kahrmann, M.,
639 Karpińska-Kołaczek, M., Kołaczek, P., Kühl, N., Kuneš, P., Lapteva, E. G., Leroy, S. A. G., Leydet,
640 M., López Sáez, J. A., Masi, A., Matthias, I., Mazier, F., Meltsov, V., Mercuri, A. M., Miras, Y.,
641 Mitchell, F. J. G., Morris, J. L., Naughton, F., Nielsen, A. B., Novenko, E., Odgaard, B., Ortu, E.,
642 Overballe-Petersen, M. V., Pardoe, H. S., Peglar, S. M., Pidek, I. A., Sadori, L., Seppä, H., Severova,
643 E., Shaw, H., Święta-Musznicka, J., Theuerkauf, M., Tonkov, S., Veski, S., van der Knaap, W. O.,
644 van Leeuwen, J. F. N., Woodbridge, J., Zimny, M., and Kaplan, J. O.: The European Modern Pollen
645 Database (EMPD) project, Veg. Hist. Archaeobot., 22, 521–530, https://doi.org/10.1007/s00334-
646 012-0388-5, 2013.

Davis, B. A. S., Chevalier, M., Sommer, P., Carter, V. A., Finsinger, W., Mauri, A., Phelps, L. N., Zanon, M., Abegglen, R., Åkesson, C. M., Alba-Sánchez, F., Anderson, R. S., Antipina, T. G., Atanassova, J. R., Beer, R., Belyanina, N. I., Blyakharchuk, T. A., Borisova, O. K., Bozilova, E., Bukreeva, G., Bunting, M. J., Clò, E., Colombaroli, D., Combourieu-Nebout, N., Desprat, S., Di Rita, F., Djamali, M., Edwards, K. J., Fall, P. L., Feurdean, A., Fletcher, W., Florenzano, A., Furlanetto, G., Gaceur, E., Galimov, A. T., Gałka, M., García-Moreiras, I., Giesecke, T., Grindean, R., Guido, M. A., Gvozdeva, I. G., Herzschuh, U., Hjelle, K. L., Ivanov, S., Jahns, S., Jankovska, V., Jiménez-Moreno, G., Karpińska-Kołaczek, M., Kitaba, I., Kołaczek, P., Lapteva, E. G., Latałowa, M., Lebreton, V., Leroy, S., Leydet, M., Lopatina, D. A., López-Sáez, J. A., Lotter, A. F., Magri, D., Marinova, E., Matthias, I., Mavridou, A., Mercuri, A. M., Mesa-Fernández, J. M., Mikishin, Y. A., Milecka, K., Montanari, C., Morales-Molino, C., Mrotzek, A., Muñoz Sobrino, C., Naidina, O. D., Nakagawa, T., Nielsen, A. B., Novenko, E. Y., Panajiotidis, S., Panova, N. K., Papadopoulou, M., Pardoe, H. S., Pędziszewska, A., Petrenko, T. I., Ramos-Román, M. J., Ravazzi, C., Rösch, M., Ryabogina, N., Sabariego Ruiz, S., Salonen, J. S., Sapelko, T. V., Schofield, J. E., Seppä, H., Shumilovskikh, L., Stivrins, N., Stojakowits, P., Svobodova Svitavska, H., Święta-Musznicka, J., Tantau, I., Tinner, W., Tobolski, K., Tonkov, S., Tsakiridou, M., et al.: The Eurasian Modern Pollen Database (EMPD), version 2, Earth Syst. Sci. Data, 12, 2423–2445, https://doi.org/10.5194/essd-12-2423-2020, 2020.

Eyring, V., Cox, P. M., Flato, G. M., Gleckler, P. J., Abramowitz, G., Caldwell, P., Collins, W. D., Gier, B. K., Hall, A. D., Hoffman, F. M., Hurtt, G. C., Jahn, A., Jones, C. D., Klein, S. A., Krasting, J. P., Kwiatkowski, L., Lorenz, R., Maloney, E., Meehl, G. A., Pendergrass, A. G., Pincus, R., Ruane, A. C., Russell, J. L., Sanderson, B. M., Santer, B. D., Sherwood, S. C., Simpson, I. R., Stouffer, R. J., and Williamson, M. S.: Taking climate model evaluation to the next level, Nat. Clim. Chang., 9, 102–110, https://doi.org/10.1038/s41558-018-0355-y, 2019.

Fick, S. E. and Hijmans, R. J.: WorldClim 2: new 1-km spatial resolution climate surfaces for global land areas, Int. J. Climatol., 37, 4302–4315, https://doi.org/10.1002/joc.5086, 2017.

Gajewski, K., Vance, R., Sawada, M., Fung, I., Gignac, L. D., Halsey, L., John, J., Maisongrande, P., Mandell, P., Mudie, P. J., Richard, P. J. H., Sherin, A. G., Soroko, J., and Vitt, D. H.: The climate of

675 North America and adjacent ocean waters ca. 6 ka. Canadian Journal of Earth Sciences 37.5: 661-
676 681, 2000.

677 Hao, Z., Phillips, T. J., Hao, F., and Wu, X.: Changes in the dependence between global precipitation
678 and temperature from observations and model simulations, Int. J. Climatol., 39, 4895–4906,
679 https://doi.org/10.1002/joc.6111, 2019.

680 He, F.: Simulating transient climate evolution of the last deglaciation with CCSM3, Ph.D. thesis,
681 University of Wisconsin-Madison, USA, 185 pp., 2010.

682 Herzschuh, U., Cao, X., Laepple, T., Dallmeyer, A., Telford, R. J., Ni, J., Chen, F., Kong, Z., Liu, G.,
683 Liu, K.-B., Liu, X., Stebich, M., Tang, L., Tian, F., Wang, Y., Wischnewski, J., Xu, Q., Yan, S., Yang,
684 Z., Yu, G., Zhang, Y., Zhao, Y., and Zheng, Z.: Position and orientation of the westerly jet
685 determined Holocene rainfall patterns in China, Nat. Commun., 10, 2376,
686 https://doi.org/10.1038/s41467-019-09866-8, 2019.

687 Herzschuh, U., Böhmer, T., Li, C., and Cao, X.: Northern Hemisphere temperature and precipitation
688 reconstruction from taxonomically harmonized pollen data set with revised chronologies using WA-
689 PLS and MAT (LegacyClimate 1.0), PANGAEA,
690 https://doi.pangaea.de/10.1594/PANGAEA.930512, 2021.

691 Herzschuh, U., Böhmer, T., Li, C., Cao, X., Hébert, R., Dallmeyer, A., Telford, R. J., Kruse, S.:
692 Reversals in temperature-precipitation correlations in the Northern Hemisphere extratropics during
693 the Holocene. Geophysical Research Letters, p.e2022GL099730,
694 https://doi.org/10.1029/2022GL099730, 2022a.

695 Herzschuh, U., Böhmer, T., Li, C., Chevalier, M., Dallmeyer, A., Cao, X., Bigelow, N. H., Nazarova,
696 L., Novenko, E. Y., Park, J., Peyron, O., Rudaya, N. A., Schlütz, F., Shumilovskikh, L. S., Tarasov,
697 P. E., Wang, Y., Wen, R., Xu, Q., and Zheng, Z.: LegacyClimate 1.0: A dataset of pollen-based
698 climate reconstructions from 2594 Northern Hemisphere sites covering the late Quaternary [Data
699 set], Zenodo, https://doi.org/10.5281/zenodo.5910989, 2022b.

700 Herzschuh, U., Li, C., Böhmer, T., Postl, A. K., Heim, B., Andreev, A. A., Cao, X., Wieczorek, M., and
701 Ni, J.: LegacyPollen 1.0: a taxonomically harmonized global late Quaternary pollen dataset of 2831

records with standardized chronologies, Earth Syst. Sci. Data, 14, 3213–3227, https://doi.org/10.5194/essd-14-3213-2022, 2022c.

Hijmans, R. J., van Etten, J., Sumner, M., Cheng, J., Baston, D., Bevan, A., Bivand, R., Busetto, L., Canty, M., Fasoli, B., Forrest, D., Ghosh, A., Golicher, D., Gray, J., Greenberg, J. A., Hiemstra, P., Hingee, K., Ilich, A., Institute for Mathematics Applied Geosciences, Karney, C., Mattiuzzi, M., Mosher, S., Naimi, B., Nowosad, J., Pebesma, E., Lamigueiro, O. P., Racine, E. B., Rowlingson, B., Shortridge, A., Venables, B., and Wueest, R.: Raster: Geographic Data Analysis and Modeling, R package version 3.5-11, https://cran.r-project.org/web/packages/raster, 2021.

Hill, M. O.: Diversity and Evenness: A Unifying Notation and Its Consequences, Ecology, 54, 427–432, https://doi.org/10.2307/1934352, 1973.

Izumi, K. and Bartlein, P. J.: North American paleoclimate reconstructions for the Last Glacial Maximum using an inverse modeling through iterative forward modeling approach applied to pollen data: Pollen-Based Climate Reconstruction, Geophys. Res. Lett., 43, 10,965-10,972, https://doi.org/10.1002/2016GL070152, 2016.

Jackson, S. T.: Pollen source area and representation in small lakes of the northeastern United States, Rev. Palaeobot. Palynol., 63, 53–76, https://doi.org/10.1016/0034-6667(90)90006-5, 1990.

Jackson, S. T. and Williams, J. W.: MODERN ANALOGS IN QUATERNARY PALEOECOLOGY: Here Today, Gone Yesterday, Gone Tomorrow?, Annu. Rev. Earth Planet. Sci., 32, 495–537, https://doi.org/10.1146/annurev.earth.32.101802.120435, 2004.

Juggins, S.: Palaeolimnological Transfer Functions: New Paradigm or Sick Science?, Quaternary International, 279–280, 228, https://doi.org/10.1016/j.quaint.2012.08.487, 2012.

Juggins, S.: rioja: Analysis of Quaternary Science Data, R package version 0.9-21, https://cran.r-project.org/web/packages/rioja, 2019.

Kaufman, D., McKay, N., Routson, C., Erb, M., Davis, B., Heiri, O., Jaccard, S., Tierney, J., Dätwyler, C., Axford, Y., Brussel, T., Cartapanis, O., Chase, B., Dawson, A., de Vernal, A., Engels, S., Jonkers, L., Marsicek, J., Moffa-Sánchez, P., Morrill, C., Orsi, A., Rehfeld, K., Saunders, K., Sommer, P. S., Thomas, E., Tonello, M., Tóth, M., Vachula, R., Andreev, A., Bertrand, S., Biskaborn, B., Bringué,

729 M., Brooks, S., Caniupán, M., Chevalier, M., Cwynar, L., Emile-Geay, J., Fegyveresi, J., Feurdean,
730 A., Finsinger, W., Fortin, M.-C., Foster, L., Fox, M., Gajewski, K., Grosjean, M., Hausmann, S.,
731 Heinrichs, M., Holmes, N., Ilyashuk, B., Ilyashuk, E., Juggins, S., Khider, D., Koinig, K., Langdon,
732 P., Larocque-Tobler, I., Li, J., Lotter, A., Luoto, T., Mackay, A., Magyari, E., Malevich, S., Mark, B.,
733 Massaferro, J., Montade, V., Nazarova, L., Novenko, E., Pařil, P., Pearson, E., Peros, M., Pienitz,
734 R., Płóciennik, M., Porinchu, D., Potito, A., Rees, A., Reinemann, S., Roberts, S., Rolland, N.,
735 Salonen, S., Self, A., Seppä, H., Shala, S., St-Jacques, J.-M., Stenni, B., Syrykh, L., Tarrats, P.,
736 Taylor, K., van den Bos, V., Velle, G., Wahl, E., Walker, I., Wilmshurst, J., Zhang, E., and Zhilich,
737 S.: A global database of Holocene paleotemperature records, Sci. Data, 7, 115,
738 https://doi.org/10.1038/s41597-020-0445-3, 2020a.

739 Kaufman, D., McKay, N., Routson, C., Erb, M., Dätwyler, C., Sommer, P. S., Heiri, O., and Davis, B.:
740 Holocene global mean surface temperature, a multi-method reconstruction approach, Sci. Data, 7,
741 201, https://doi.org/10.1038/s41597-020-0445-3, 2020b.

742 Li, C., Postl, A. K., Böhmer, T., Cao, X., Dolman, A. M., and Herzschuh, U.: Harmonized chronologies
743 of a global late Quaternary pollen dataset (LegacyAge 1.0), Earth Syst. Sci. Data, 14, 1331–1343,
744 https://doi.org/10.5194/essd-14-1331-2022, 2022.

745 Liu, Z., Zhu, J., Rosenthal, Y., Zhang, X., Otto-Bliesner, B. L., Timmermann, A., Smith, R. S., Lohmann,
746 G., Zheng, W., and Timm, O. E.: The Holocene temperature conundrum, PNAS, 111, E3501–E3505,
747 https://doi.org/10.1073/pnas.1407229111, 2014.

748 Marcott, S. A., Shakun, J. D., Clark, P. U., and Mix, A. C.: A Reconstruction of Regional and Global
749 Temperature for the Past 11,300 Years, Science, 339, 1198–1201,
750 https://doi.org/10.1126/science.1228026, 2013.

751 Marsicek, J., Shuman, B. N., Bartlein, P. J., Shafer, S. L., and Brewer, S.: Reconciling divergent trends
752 and millennial variations in Holocene temperatures, Nature, 554, 92–96,
753 https://doi.org/10.1038/nature25464, 2018.

754 Mauri, A., Davis, B. A. S., Collins, P. M., and Kaplan, J. O.: The climate of Europe during the Holocene:
755 a gridded pollen-based reconstruction and its multi-proxy evaluation, Quat. Sci. Rev., 112, 109–
756 127, https://doi.org/10.1016/j.quascirev.2015.01.013, 2015.

Nychka, D., Furrer, R., Paige, J., Sain, S., Gerber, F., and Iverson, M.: fields: Tools for Spatial Data, R package version 10.3, https://cran.r-project.org/web/packages/fields/index.html, 2020.

Oksanen, J., Blanchet, F. G., Friendly, M., Kindt, R., Legendre, P., McGlinn, D., Minchin, P. R., O'Hara, R. B., Simpson, G. L., Solymos, P., Stevens, M. H. H., Szoecs, E., and Wagner, H.: Vegan: Community Ecology Package, R package version 2.5-7, https://cran.r-project.org/web/packages/vegan, 2020.

Overpeck, J. T., Webb, T., and Prentice, I. C.: Quantitative Interpretation of Fossil Pollen Spectra: Dissimilarity Coefficients and the Method of Modern Analogs, Quat. Res., 23, 87–108, https://doi.org/10.1016/0033-5894(85)90074-2, 1985.

Parnell, A. C., Haslett, J., Sweeney, J., Doan, T. K., Allen, J. R. M., and Huntley, B.: Joint palaeoclimate reconstruction from pollen data via forward models and climate histories, Quaternary Science Reviews, 151, 111–126, https://doi.org/10.1016/j.quascirev.2016.09.007, 2016.

R Core Team: R: A language and environment for statistical computing, R Foundation for Statistical Computing, Vienna, Austria, available online at: https://www.R-project.org/, 2020.

Rehfeld, K., Trachsel, M., Telford, R. J., and Laepple, T.: Assessing performance and seasonal bias of pollen-based climate reconstructions in a perfect model world, Clim. Past, 12, 2255–2270, https://doi.org/10.5194/cp-12-2255-2016, 2016.

Routson, C. C., McKay, N. P., Kaufman, D. S., Erb, M. P., Goosse, H., Shuman, B. N., Rodysill, J. R., and Ault, T.: Mid-latitude net precipitation decreased with Arctic warming during the Holocene, Nature, 568, 83–87, https://doi.org/10.1038/s41586-019-1060-3, 2019.

Simpson, G. L.: Analogue Methods in Palaeolimnology, in: Tracking Environmental Change Using Lake Sediments: Data Handling and Numerical Techniques, edited by: Birks, H. J. B., Lotter, A. F., Juggins, S., and Smol, J. P., Springer Netherlands, Dordrecht, 495–522, https://doi.org/10.1007/978-94-007-2745-8_15, 2012.

Simpson, G. L., Oksanen, J., Maechler, M.: analogue: Analogue and Weighted Averaging Methods for Palaeoecology, R package version 0.17-6, https://cran.r-project.org/web/packages/analogue, 2021.

784 Sugita, S.: A Model of Pollen Source Area for an Entire Lake Surface, Quat. Res., 39, 239–244,
785 https://doi.org/10.1006/qres.1993.1027, 1993.

786 Tarasov, P. E., Nakagawa, T., Demske, D., Österle, H., Igarashi, Y., Kitagawa, J., Mokhova, L.,
787 Bazarova, V., Okuda, M., Gotanda, K., Miyoshi, N., Fujiki, T., Takemura, K., Yonenobu, H., and
788 Fleck, A.: Progress in the reconstruction of Quaternary climate dynamics in the Northwest Pacific:
789 A new modern analogue reference dataset and its application to the 430-kyr pollen record from
790 Lake Biwa, Earth Sci. Rev., 108, 64–79, https://doi.org/10.1016/j.earscirev.2011.06.002, 2011.

791 Telford, R. J.: palaeoSig: Significance Tests for Palaeoenvironmental Reconstructions, R package
792 version 2.0-3, https://cran.r-project.org/web/packages/palaeoSig, 2019.

793 Telford, R. J. and Birks, H. J. B.: A novel method for assessing the statistical significance of
794 quantitative reconstructions inferred from biotic assemblages, Quat. Sci. Rev., 30, 1272–1278,
795 https://doi.org/10.1016/j.quascirev.2011.03.002, 2011.

796 ter Braak, C. J. F.: CANOCO - a FORTRAN program for canonical community ordination by (Partial)
797 (Detrended) (Canonical) correspondence analysis and redundancy analysis. Agricultural
798 Mathematics Group, Wageningen, 1988.

799 ter Braak, C. J. F. and Juggins, S.: Weighted averaging partial least squares regression (WA-PLS):
800 an improved method for reconstructing environmental variables from species assemblages,
801 Hydrobiologia, 269, 485–502, https://doi.org/10.1007/BF00028046, 1993.

802 Tian, F., Cao, X., Dallmeyer, A., Zhao, Y., Ni, J., and Herzschuh, U.: Pollen-climate relationships in
803 time (9 ka, 6 ka, 0 ka) and space (upland vs. lowland) in eastern continental Asia, Quat. Sci. Rev.,
804 156, 1–11, https://doi.org/10.1016/j.quascirev.2016.11.027, 2017.

805 Trachsel, M. and Telford, R. J.: All age–depth models are wrong, but are getting better, Holocene, 27,
806 860–869, https://doi.org/10.1177/0959683616675939, 2017.

807 Trenberth, K. E.: Changes in precipitation with climate change, Clim. Res., 47, 123–138,
808 https://doi.org/10.3354/cr00953, 2011.

809 Whitmore, J., Gajewski, K., Sawada, M., Williams, J. W., Shuman, B., Bartlein, P. J., Minckley, T.,
810 Viau, A. E., Webb, T., Shafer, S., Anderson, P., and Brubaker, L.: Modern pollen data from North
811 America and Greenland for multi-scale paleoenvironmental applications, Quat. Sci. Rev., 24, 1828–
812 1848, https://doi.org/10.1016/j.quascirev.2005.03.005, 2005.

813 Williams, J. W., Grimm, E. C., Blois, J. L., Charles, D. F., Davis, E. B., Goring, S. J., Graham, R. W.,
814 Smith, A. J., Anderson, M., Arroyo-Cabrales, J., Ashworth, A. C., Betancourt, J. L., Bills, B. W.,
815 Booth, R. K., Buckland, P. I., Curry, B. B., Giesecke, T., Jackson, S. T., Latorre, C., Nichols, J.,
816 Purdum, T., Roth, R. E., Stryker, M., and Takahara, H.: The Neotoma Paleoecology Database, a
817 multiproxy, international, community-curated data resource, Quat. Res., 89, 156–177,
818 https://doi.org/10.1017/qua.2017.105, 2018.

819 Williams, J. W., Webb III, T., Richard, P. H., and Newby, P.: Late Quaternary biomes of Canada and
820 the eastern United States, J. Biogeogr., 27, 585–607, https://doi.org/10.1046/j.1365-
821 2699.2000.00428.x, 2000.

822 Wu, R., Chen, J., and Wen, Z.: Precipitation-surface temperature relationship in the IPCC CMIP5
823 models, Adv. Atmos. Sci., 30, 766–778, https://doi.org/10.1007/s00376-012-2130-8, 2013.